Russian Chemical Reviews **75** (12) 1065 – 1082 (2006) © 2006 Russian Academy of Sciences and Turpion Ltd

DOI 10.1070/RC2006v075n12ABEH003637

Inorganic nanofluorides and related nanocomposites

S V Kuznetsov, V V Osiko, E A Tkatchenko, P P Fedorov

Contents

I.	Introduction	1065
II.	Hydrolysis of fluorides and its prevention	1066
III.	Synthesis of nanoparticles	1067
IV.	One-dimensional nanoobjects	1073
V.	Two-dimensional nanoobjects	1073
VI.	Fluoride nanocomposites	1074
VII.	Nanotechnology and nanoarchitecture	1078
VIII.	Conclusion	1078

Abstract. The properties and prospects of application of fluoride nanoparticles are discussed. Pyrohydrolysis is considered as the key process determining the chemistry and technology of fluorides; its role increases on going to the nanosize region. The physical and chemical methods for the synthesis of fluoride nanoparticles, one- and two-dimensional nanoobjects as well as approaches to the preparation of nanocomposites (glass ceramics, heterovalent solid solutions with defect clusters, eutectoid composites, *etc*.) are analysed. Nanotechnology techniques used to produce heterogeneous nanoobjects are outlined. The bibliography includes 238 references.

I. Introduction

In recent years, nanosized particles have attracted increasing interest due to their unique physical and chemical properties, which differ from the properties of macro- and microparticles. However, nanoparticles of inorganic fluorides have received less attention than nanoparticles of other classes of compounds such as metals, oxides and semiconductors. In particular, nanoparticles of inorganic fluorides were not mentioned in the handbook [1] and only one of 668 references in the review [2] refers to fluorides. Major publications on fluoride nanoparticles appeared in the last 5 years.

The synthesis and investigations of fluoride nanoparticles are of interest for to the following reasons.

Laser ceramics was developed based on yttrium aluminium garnet and rare-earth oxides. The optical transmission, optical losses and spectral-generation characteristics of this ceramics are not virtually inferior to those of single crystals.[3,4] Considerable progress in the nanoparticle preparation technology was achieved with the use of self-organisation processes of nanoparticles. The advantages of laser nanoceramics over single crystals include the possibility of producing large objects, improved mechanical characteristics, uniform distribution and high concentrations of activating ions and the possibility of preparing a transparent optical medium where the synthesis of single crystals presents problems.

Analysis of the trends of development of modern photonics in different countries demonstrated that devices based on fluoride compounds will play a considerable role in the nearest future. This statement is supported by the following physical facts:

— transmission of fluorides in a wide spectral region (from 0.2 to 6 μm); short phonon spectra preventing the development of the adverse effect of multiphonon relaxation in electronic levels of impurity ions;

— the ease of introduction of considerable amounts of active rare-earth ions (up to concentrations of 10^{21} cm^{-3}) into fluorides;

— better mechanical properties and higher moisture resistance of fluorides compared to other classes of compounds having a wide transmission window, such as chlorides and chalcogenides;

— high thermal conductivity of fluorides.

Due to the above-mentioned advantages, fluorides, primarily as single crystals, are successfully used for the production of active and passive elements of laser systems employed in medicine, ecology and informatics, in particular, as elements of unique tunable lasers.

In the light of the above, the possibility of constructing analogous fluoride nanoceramics for photonics (lasers, scintillators, *etc*.) primarily based on alkaline-earth fluorides doped with rare-earth metals is very attractive.[5–8]

Certain parameters of nanoparticles are improved compared to bulk crystals. The special spectroscopic properties of nanoparticles containing lanthanide ions are determined by the following circumstances:[9–12]

— the absence of low-energy phonons and low density of phonons resulting in a radical change in the dynamics of energy transfer;

— a change in local symmetry of cations in small clusters and on the particle surface;

— small Stark splitting due to a decrease in the crystal field strength.

These features are responsible for the specific nature and prospects of development of nanophotonics. In particular, the luminescence intensity and the lifetime of the excited state for a nanocrystalline $NaGdF_4:Eu^{3+}$ powder increase with a decrease in particle size from 60 to 14 nm.[11] Thus, nanopowders of various

S V Kuznetsov, V V Osiko, E A Tkatchenko, P P Fedorov Laser Materials and Technologies Research Centre, A M Prokhorov General Physics Institute, Russian Academy of Sciences, ul.Vavilova 38, 119991 Moscow, Russian Federation. Fax (7-495) 135 77 44, e-mail: tez@rambler.ru (S V Kuznetsov), tel. (7-495) 135 77 44, e-mail: osiko@lst.gpi.ru (V V Osiko), e-mail: tkatchenko@ns.crys.ras.ru (E A Tkatchenko), tel. (7-499) 503 82 76, e-mail: ppf@lst.gpi.ru (P P Fedorov)

Received 19 March 2006
Uspekhi Khimii **75** (12) 1193 – 1211 (2006); translated by T N Safonova

fluorides doped with lanthanide ions hold promise for the production of monitor displays, optical amplifiers, lasers and phosphors.[11, 13–15]

Sodium fluoride nanoparticles doped with uranium exhibit much higher electron emission than single crystals, due to which these nanoparticles were recommended as materials for probes for cytological, microbiological and medical studies.[16]

Fluoride nanoparticles, to be more precise, powders with very high specific surface area (up to 200 $m^2\ g^{-1}$ and larger) have attracted interest as materials for new types of catalysts. Due to high specific surface area, fluorides can serve as very efficient acid catalysts because coordinatively unsaturated sites of metal atoms are accumulated on the surface of such compounds.[17, 18] Powders of fluorides AlF_3, 'AlClF', FeF_3 and CrF_3 with highly developed surface act as very strong Lewis acids, which are comparable in or even stronger than SbF_5. Nanocrystalline magnesium fluoride can be used as a sorbent (support).[17–21] The catalytic activity is particularly high if compounds are amorphous.

In some cases, the synthesis of fluoride nanoparticles is simpler, more efficient and is characterised by a higher output compared to conventional methods for the preparation of single and polycrystals (sintering or fusion of precursors at high temperature in a fluorinating atmosphere). In particular, this is true for the synthesis of complex fluorides by precipitation from solutions, which does not require complicated apparatus. The preparation of powders in the sol–gel process occurs much more rapidly than in the solid-phase synthesis, which was exemplified by $BaMgF_4$ and $SrAlF_5$ as promising nonlinear optical crystals for laser frequency conversion to the UV range.[22]

Fluoride nanoparticles possess enhanced reactivity due to which the temperature of solid-phase reactions with their involvement can be lowered.

Composites containing nanocrystalline lithium fluoride and a conducting phase (carbon or metals) were patented as electrode materials for reversible lithium batteries.[23]

Nanoparticles of calcium fluorophosphates favour remineralisation of tooth enamel thus preventing caries and tooth eruption and improving the quality of tooth fillings.[24, 25] The addition of YbF_3 (as well as $BaSO_4$) nanoparticles to dental cements improves their mechanical characteristics.[26]

Nanocomposites, among which are fluoride glasses and heterovalent solid solutions primarily of alkaline-earth and rare-earth fluorides, are polyfunctional materials and have wide application.

Nanotechnology enables synthesis of compounds in a highly non-equilibrium state. In particular, $NaYF_4$ (a high-temperature cubic modification, which is transformed into an equilibrium low-temperature modification with time)[27] and BaY_2F_8 (Ref. 28) were prepared as unstable crystal polymorphs. In nanotechnology, classical manifestations of the Ostwald step rule can be observed.

The boundary that determines the transition of a substance into the nanostate can be drawn in different ways based on different physical properties. In the present review, this concept is extended and referred to particles with size up to 100 nm; the specific surface area of spherical nanoparticles with this diameter and a density of 6 g cm^{-3} is higher than 10 $m^2\ g^{-1}$.

In addition to ensembles of nanoparticles, there are nanostructured objects with well-developed porosity and, correspondingly, with high specific surface area in which individual particles are difficult to distinguish. Amorphous fluoride catalysts belong to such objects,[17–21] and they are also considered in the present review.

We focus our attention on procedures for the preparation of nanosized fluoride materials as powders and composites. The methods for characterisation of such materials are beyond the scope of the present review. The properties and fields of application and methods for the synthesis of one- and two-dimensional nanoobjects are briefly outlined.

II. Hydrolysis of fluorides and its prevention

Fluorides react with water with elimination of HF, which causes difficulties in the preparation of both bulk fluoride materials and nanoparticles. This process occurring at high temperature is called pyrohydrolysis.[29–35] The first step of pyrohydrolysis involves adsorption of water molecules on the surface of fluoride particles. In the next steps, the fluoride ion is replaced by OH^- and O^{2-} anions according to the reactions

$$F^- + H_2O \longrightarrow OH^- + HF\uparrow, \quad (1)$$

$$2\,F^- + H_2O \longrightarrow O^{2-} + 2\,HF\uparrow. \quad (2)$$

Due to the similar sizes of the fluoride ion and the hydroxyl anion, the replacement of the former by the latter occurs by a mechanism of isomorphic substitution, the single-phase state of the system being retained. Once the critical concentration is achieved, accumulation of oxygen ions in the lattice of bulk fluoride samples leads to formation of the second phase (oxide or oxofluoride). In particular, pyrohydrolysis of rare-earth trifluorides LnF_3 initially affords oxofluorides with different compositions (Ln_2OF_4, $Ln_4O_3F_6$, LnOF, *etc.*). Oxides are the final transformation products of LnF_3

$$4\,LnF_3 + 3\,H_2O \longrightarrow Ln_4O_3F_6 + 6\,HF\uparrow, \quad (3)$$

$$LnF_3 + H_2O \longrightarrow LnOF + 2\,HF\uparrow, \quad (4)$$

$$2\,LnOF + H_2O \longrightarrow Ln_2O_3 + 2\,HF\uparrow. \quad (5)$$

It should be noted that the replacement of the fluorine atom by the oxygen atom is thermodynamically unfavourable. Hence, fluorides are generally stable in dry air (oxygen) even on heating.

Pyrohydrolysis starts on the surface of a substance and continues in the bulk (Fig. 1 *a*). The rate of the process depends on the diffusion coefficients of anions. In bulk samples, the oxygen diffusion rates along lattice defects (dislocations and intergrain boundaries) are substantially higher (Fig. 1 *b*). Lattice defects can be decorated with the second oxide phase. An increase in the surface area and the passage to nanoparticles would lead to sharp acceleration of this process. The probable scheme of pyrohydrolysis of nanoparticle agglomerates is shown in Fig. 1 *c*. Rapid and spatially complicated pyrohydrolysis processes apparently occur in the case of a fractal structure of nanoparticles.

Fluorides differ substantially in the tendency to undergo pyrohydrolysis. These compounds are characterised by such

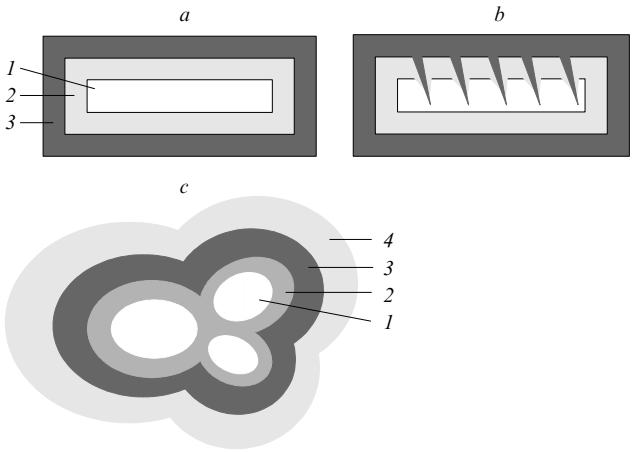


Figure 1. Scheme of pyrohydrolysis of a fluorite single crystal. (*a*): (*1*) A single crystal, (*2*) an intermediate opalescent zone, (*3*) a non-transparent outer zone (oxide phase);[34] (*b*) the same in the presence of dislocation bundles in the crystal; (*c*) the same in the case of hydrolysis of a nanoparticle agglomerate: (*1*) fluoride, (*2*) hydroxofluoride, (*3*) oxofluoride, (*4*) a layer of adsorbed water.

parameters as the temperature at which hydrolysis starts or the time of completion of hydrolysis at a particular temperature, which are purely empirical. It was found [32] that the stability of fluorides with respect to pyrohydrolysis decreases in the following order: $NaF > SrF_2 > BaF_2 > LiF > CaF_2 > MgF_2 > LnF_3 > AlF_3 > BiF_3 > ZnF_2 > ThF_4 > UF_4$. The time required for complete hydrolysis at 1000 °C is longer than 20 min for alkali, alkaline-earth (except for magnesium) and beryllium fluorides; the time for other fluorides is shorter than 20 min. The hydrolytic stability of LnF_3 decreases on going from light lanthanides to heavy lanthanides.[33,35] The abnormally high pyrohydrolysis rate is observed for CeF_3.[33,36] According to the results of a study,[31] fluorides can be arranged in the following series of decreasing stability to hydrolysis: BaF_2, $CaF_2 > MgF_2 > MnF_2$, $PbF_2 > CdF_2 > CoF_2 > NiF_2 > ZnF_2 > FeF_2$, $CrF_3 > FeF_3$, CuF_2, AgF. In another study,[37] the following series was proposed (based on the temperature at which the reaction between a fluoride powder and a superheated water vapour starts): $BaF_2 > SrF_2 > CaF_2 > MgF_2 > CdF_2 > ZnF_2$. For strontium fluoride, this temperature is 1120 °C; for zinc fluoride, 400 °C.

Hydrolysis of some fluorides starts at room temperature. In particular, it was found [38] that prolonged (for several years) storage of an indium fluoride powder in air is accompanied not only by hydration but also by hydrolysis. Zirconium and hafnium fluorides behave analogously. Hydrolysis of highly hygroscopic niobium pentafluoride occurs even more readily and it is recommended to employ hydrogen fluoride liberated upon its exposure in air at room temperature for preparative purposes.[39]

Fluorides are characterised by strong water vapour adsorption on the surface.[40,41] An increase in the powder dispersity and passage to nanoparticles would lead to a sharp decrease in the temperature at which hydrolysis starts and an increase in the number of fluorides hydrolysable at room temperature.

Ordinary powders prepared from aqueous solutions or containing surface-adsorbed moisture are dehydrated by heating to a temperature lower than the temperature at which hydrolysis starts (for example, heating in high vacuum to 200 °C). Technological operations are also carried out in the atmosphere of anhydrous inert gas. In some cases, the use of high vacuum is insufficient to prevent pyrohydrolysis in high-temperature technological processes. An active fluorinating atmosphere (pyrolysis products of Teflon, hydrogen fluoride, tetrafluoromethane or their combinations) is used.[29] The efficiency of gaseous fluorinating reagents decreases in the following series: $C_2F_4 > NF_3 > CF_4 > COF_2 > SF_6$.[42]

III. Synthesis of nanoparticles

1. Synthesis of nanoparticles by physical methods

a. Vapour phase deposition

Initial steps of the formation of thin films (formation of adatoms, critical nuclei and growth islets), including evaporation (sublimation) of a substance onto a substrate, belong to the field of nanotechnology. Nanoparticles which are formed in the vapour bulk by a mechanism of homogeneous nucleation, can be collected. Nanoparticles of PbF_2 of both cubic and orthorhombic polymorphs (21–43 nm) were synthesised by vapour condensation in ultrahigh vacuum.[43] Calcium fluoride nanoparticles were synthesised analogously.[44]

b. Mechanical grinding

Fluoride nanoparticles can be synthesised using high-energy mills. Images of LiF particles obtained by scanning electronic and atomic force microscopy are shown in Figs. 2 *a*,*c* and 2 *b*,*d*, respectively. Nanoparticles of a sample ground in ethanol in an agate mortar are presented in Fig. 2 *a*,*b*. An increase in the time of grinding leads to such a compact particle agglomeration that scanning electronic microscopy does not reveal details of the particle structure (Fig. 2 *c*). However, atomic force microscopy reveals fitting of particles, each particle having an irregular shape and, apparently, being an agglomeration product of several nanoparticles (Fig. 2 *d*). It should be noted that there are no planar (001) faces, which are very typical of lithium fluoride micropowders due to perfect cleavage.†

Calcium fluoride nanoparticles with a size of 15–20 nm were prepared by grinding single crystals in an agate mortar under a layer of acetone followed by ultrasonic dispersion.[45]

Nanoparticles of FeF_3 and GaF_3 were prepared [46,47] by mechanical milling using zirconium oxide balls in a high-energy mill under argon for 16–20 h. Studies by powder X-ray diffraction, Mössbauer spectroscopy and NMR spectroscopy demonstrated that nanocrystalline grains with a size of ~15 nm held together by disordered intergrain layers were formed. The magnetic properties of FeF_3 and GaF_3 nanopowders are similar to those of amorphous phases.

c. Laser ablation

The energy can be pumped into a substance also by laser ablation. For example, a procedure for the synthesis of nanoparticles by ablation of a sodium fluoride single crystal doped with uranium onto a molybdenum support was documented.[16] The nanoparticle size was 20–30 nm.

2. Synthesis of nanoparticles by chemical methods

a. Thermolysis of precursors

Salts of fluoroorganic acids, primarily, of trifluoroacetic acid can be used for the synthesis of fluorides by thermolysis. Under particular reaction conditions, highly dispersed samples with high specific surface area can be prepared. The preliminary synthesis of salts was carried out by the reactions of trifluoroacetic acid with the corresponding hydroxides or carbonates, for example, according to the reactions

$$CaCO_3 + 2\,CF_3CO_2H \longrightarrow Ca(CF_3COO)_2 \cdot H_2O + CO_2\uparrow, \quad (6)$$

$$Sr(OH)_2 + 2\,CF_3CO_2H \longrightarrow Sr(CF_3COO)_2 \cdot 2\,H_2O. \quad (7)$$

Decomposition of trifluoroacetates can be accompanied by the formation of a solid carbon phase, for example, according to the reaction

$$Sr(CF_3COO)_2 \cdot 2\,H_2O \longrightarrow SrF_2 + CF_4\uparrow + C + 2\,CO_2\uparrow + 2\,H_2O\uparrow. \quad (8)$$

Decomposition can be carried out in an inert atmosphere under dynamic vacuum, by the flux method and by chemical vapour phase deposition. Fluoroacetic acid is used as a fluorinating reagent in the sol–gel process. In this case, the synthesis of fluoroacetates is followed by their decomposition.

Decomposition of trifluoroacetates in air affords oxyfluoride phases. For example, study of pyrolysis of yttrium trifluoroacetate on a quartz glass surface in the temperature range of 400–900 °C showed [48] that the initially formed YF_3 particles are successively transformed into $YO_{0.80}F_{1.40}$ (orthorhombic system), YOF (trigonal system) and Y_2O_3, which corresponds to pyrohydrolysis of bulk samples. Only oxofluorides were obtained [49] by decomposition of lanthanum trifluoroacetate in a SiO_2 matrix. Oxofluorides are also formed if a basic salt, for example, $InOH(CF_3COO)_2$,[50] is obtained in the initial synthesis of trifluoroacetates.

Aluminium and chromium trifluoroacetates were used as precursors [21] to give aluminium and chromium fluoride powders with specific surface area up to 50 $m^2\ g^{-1}$. Thermolysys of europium trifluoroacetate in a melt of trioctylphosphine oxide afforded [51] EuF_3 nanoparticles with a size of 3–10 nm.

Alkaline-earth (barium, strontium and calcium) fluorides with highly developed specific surface were synthesised [52] by thermolysis of trifluoroacetates of the corresponding metals in an inert

† P P Fedorov, S V Kuznetsov, V A Konyushkin, S V Petrov, V G Kuryavyi, V N Buznik, S V Lavrishchev, in *The XIIth National Conference on Crystal Growth (NCCG-2006) (Abstracts of Papers)* (Moscow: Institute of Crystallography of the Russian Academy of Sciences, 2006) p. 417.

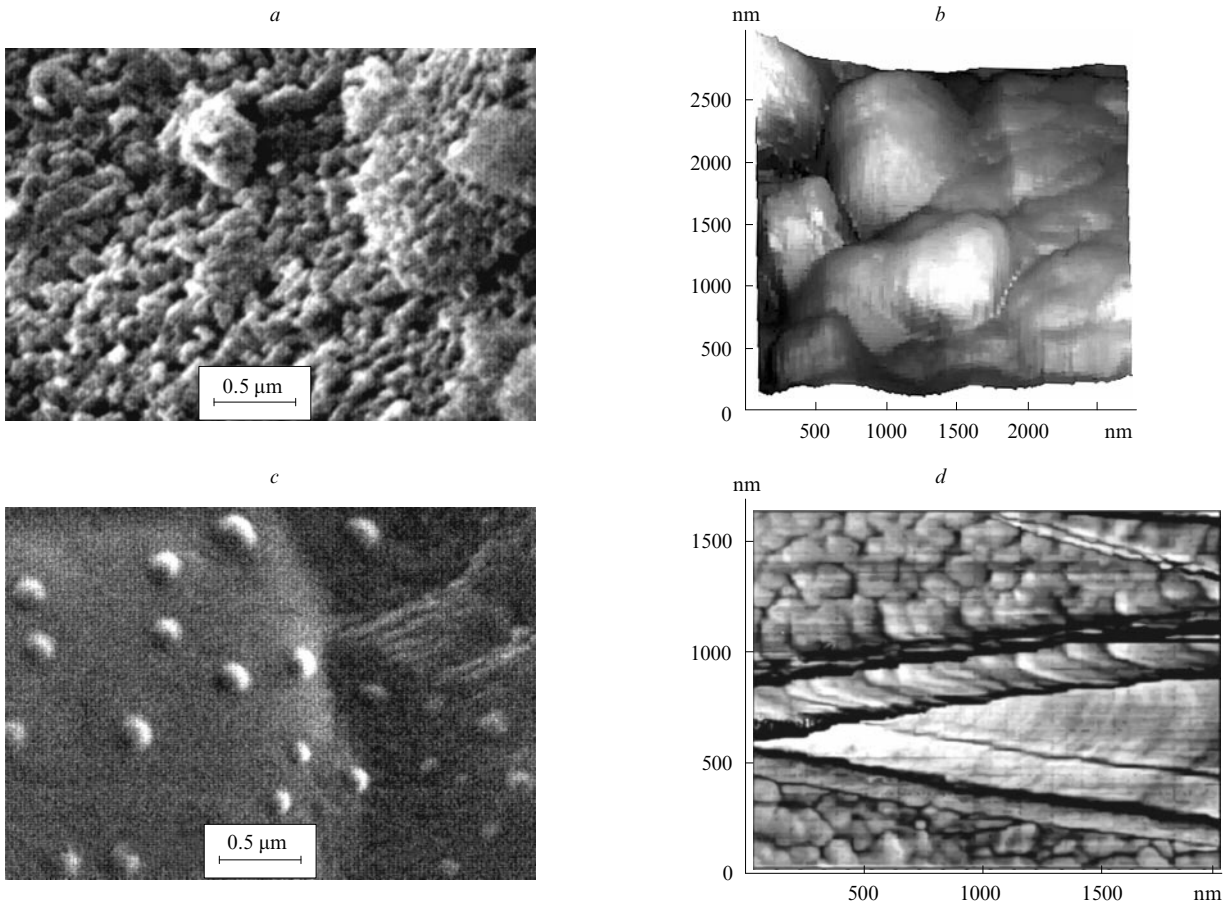


Figure 2. Photomicrographs of LiF particles after grinding of a single crystal in ethanol in an agate mortar.
(*a*, *b*) Manual grinding for 2 h (courtesy of S V Lavrishchev, the Research Centre of Fibre Optics at the A M Prokhorov General Physics Institute of the Russian Academy of Sciences); (*c*, *d*) grinding in a FRITSCH-Pulverizette 00.502 mill for 5 h (courtesy of V G Kuryavyi, the Institute of Chemistry of the Far-Eastern Branch of the Russian Academy of Sciences).

atmosphere followed by annealing under a stream of oxygen at 500 °C (to burn off carbon impurities). The specific surface areas of the resulting CaF_2, SrF_2 and BaF_2 samples were 44, 37 and 24 $m^2\ g^{-1}$, respectively. The results of studies of the SrF_2 surface by scanning electronic microscopy are presented in Fig. 3.

Fluorides can be synthesised in addition to thermolysis of trifluoroacetates by transformations of other fluoroorganic compounds. For example, four fluoroorganic compounds were studied [53] with the aim of preparing thin films of NaF by chemical vapour phase deposition. The best results were obtained with the use of sodium hexafluoroisopropoxide $(CF_3)_2CHONa$. Fluoroalkoxides were used in the synthesis of fluorides by chemical vapour phase deposition.[54] Anhydrous lanthanum hexafluoroacetylacetonate served as a precursor [55] for the preparation of nanosized-thick films of LaF_3 by organometallic chemical vapour deposition. Heating of bis(trifluoromethanesulfonyl)imide, $(CF_3SO_2)_2NH$, in a SiO_2 matrix at 400 °C afforded LaF_3.[49]

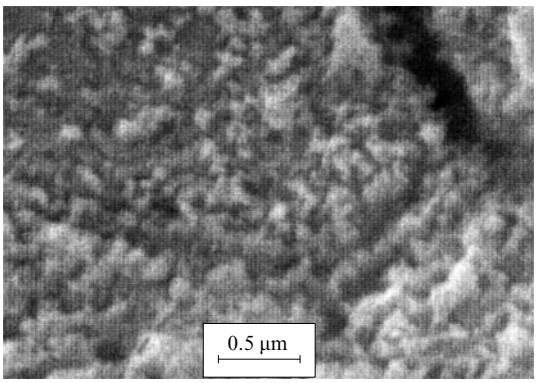


Figure 3. Electronic image of strontium fluoride after decomposition of trifluoroacetate.[52]
The specific surface area is 37 $m^2\ g^{-1}$.

Heating of a fluorine-containing gel prepared by hydrolysis of alkaline-earth and rare-earth fluoroalkoxides afforded pure fluorides, the particle size depends on the conditions of thermal treatment.[56]

Different in principle precursors are documented.[57] Nanoparticles of rare-earth fluorides (Ln = Nd, Sm, Eu, Gd and Tb) were synthesised by decomposition of needle-like NH_4LnF_4 particles, precipitated from methanolic solutions according to the reaction

$$NH_4LnF_4 \longrightarrow LnF_3 + NH_3\uparrow + HF\uparrow. \qquad (9)$$

Decomposition products retained the shape of the precursor particles.

b. Mechanochemical synthesis

In some cases, mechanical milling of a mixture of fluorides in high-energy mills is accompanied by chemical reaction producing nanoparticles.[58] In a number of publications, the formation of submicrometre-sized particles was reported. However, these particles are presumably agglomerated from smaller particles, and we include these data in the present review. Experiments [59–62] were

performed with the use of a planetary ball mill with zirconium oxide balls 15 mm in diameter at a rotation speed of 700 rpm. Milling was carried out at room temperature.

Oxofluorides LnOF with a particle size of 15–20 nm were synthesised from a mixture of oxides and fluorides (the reaction time was 1–2 h).[59]

Complex fluorides $MLnF_4$ ($LiYF_4$, KYF_4 and $NaLnF_4$, where Ln = Y, Pr, Nd, Gd, Ho or Er) were synthesised[58] by the mechanochemical solid-phase reaction of MF and LnF_3 powders. The completeness of the reaction was determined from powder X-ray diffraction data and the amount of unconsumed MF dissolved in water. The reaction was completed in 4 h. The size of coherent scattering regions of the resulting particles estimated from line broadening in X-ray diffraction patterns was 13 nm, which is consistent with the results of scanning electron microscopy.

Cubic perovskites $KM^{II}F_3$ (M^{II} = Mg, Ca, Mn, Fe, Co, Ni and Zn) were prepared by milling equimolar amounts of KF and the corresponding difluoride in a planetary mill in air.[61] The synthesis was completed in 6 h. Study by scanning electron microscopy demonstrated that large agglomerates with a particle size of ~200 nm were obtained. The absence of the evidence of hydrolysis was unexpected taking into account high hygroscopicity of KF and the fact that transition metal fluorides are easily hydrolysed. The lattice parameters of the resulting compounds are similar to the corresponding characteristics of specimens prepared by the solid-phase synthesis. Metal–oxygen bonds were not found by X-ray photoelectron spectroscopy.

The reaction of lanthanum oxide with polytetrafluoroethylene was studied.[60] After milling for 4 h, the product consisted of oxofluoride LaOF, amorphous $La(CO_3)F$ and carbon. Heating in air to 600 °C afforded pure LaOF with a particle size of ~10 nm.

Nanocrystals of a non-stoichiometric fluorite phase $Ca_{1-x}La_xF_{2+x}$ were prepared by the mechanochemical synthesis from a mixture of single crystals consisting of CaF_2 with an additive of 20 (or 10) mol.% LaF_3.[63] The components were ground in a planetary ball mill under argon. The reaction started after milling for 30 min. Milling for 2 h did not lead to completion of the reaction (90%–95% yield). The coherent scattering regions were 8–30 nm. After heating to 1000 °C, nanoparticles of the solid solution $Ca_{0.8}La_{0.2}F_{2.2}$ decomposed to give two fluorite phases with composition $Ca_{0.52}La_{0.48}F_{2.48}$ and $Ca_{0.94}La_{0.06}F_2$, which does not correspond to the phase diagram.

The mechanochemical synthesis of fluorine-conducting solid electrolytes ($Pb_{1-x}Sn_xF_2$ and $NH_4Sn_2F_5$) was documented.[64]

Ball milling was used to introduce a small amount of a metal catalyst (iron or nickel) into magnesium hydride by the reaction with fluorides.[65–67] The resulting substance is a promising material for hydrogen power engineering. Mixing of preground MgH_2 and FeF_3 (or NiF_2) powders followed by milling affords MgF_2 nanoparticles, which prevent hydride particle agglomeration. Both primary and secondary milling is performed in an inert atmosphere. Nanofluoride particles can also have a catalytic effect on hydrogen sorption.

c. Precipitation from solutions

Fluorides of many metals are poorly soluble in water. The synthesis of fluorides by the exchange reactions with precipitation of the product has long been known. Precipitation of rare-earth trifluorides was examined in detail.[68] Precipitation of phases formed in $KF–LnF_3$ systems from aqueous solutions[69–71] and in $NaF–LnF_3$ systems is documented.[69–73] Relatively recently, it has been found that nanoparticles can be synthesised according to this procedure, although the formation of, for example, colloidal solutions of $NH_4Y_3F_{10}$ and $NH_4Y_2F_7$ by the reactions of YCl_3 and NH_4HF_2 solutions was documented.[74]

Compounds $NaLnF_4$ (Ln = Y or Yb) doped with praseodymium ions were synthesised by mixing chloride solutions (prepared by dissolution of rare-earth oxides in boiling hydrochloric acid) with stoichiometric amounts of a NaF hot solution.[27] The precipitate was repeatedly washed with distilled water and dried at 80 °C. The initially formed high-temperature cubic modification passed completely into the hexagonal modification (a = 5.969, c = 3.53 Å) after ageing of the precipitate for 10 days. The average grain size of these phases was ~900 nm.

This procedure was subject to modifications.[11, 14, 28, 75] Spherical $NaGdF_4:Eu^{3+}$ nanoparticles of a size of 20 nm (data from transmission electron microscopy) were prepared by precipitation. Storage of the powder at 650 °C under a stream of Ar + 10% SF_6 led to an increase in the particle size to 50–350 nm. No oxygen impurities were revealed by IR spectroscopy and Eu^{3+} ion spectroscopy.[11, 75] $KGdF_4:Eu^{3+}$ nanoparticles were synthesised analogously;[14] the size of coherent scattering regions of the particles was 19 nm. A metastable cubic modification was precipitated. Heating led to a complex change of structural types, and the $KErF_4$-type hexagonal modification was obtained for the first time.[76] The presence of the hydroxyl ion was revealed by IR spectroscopy. The non-equilibrium polymorph $BaY_2F_8:Eu^{3+}$ (as a nanopowder) with a fluorite-type structure and the lattice parameter a = 5.767 Å was synthesised analogously.[28] This lattice parameter is substantially smaller than that of any equilibrium composition of the solid solution $Ba_{1-x}Y_xF_{2+x}$ in the $BaF_2–YF_3$ system.[77] Upon heating in a stream of Ar + 10% SF_6, the sample undergoes a phase transition to the equilibrium monoclinic structure BaY_2F_8.

In an analogous solution precipitation method,[78] aqueous solutions of $Eu(NO_3)_3 \cdot 6H_2O$ and NaF served as the starting compounds. The reaction product that formed upon mixing of these two solutions was washed with water and ethanol and dried at 70 °C for 3 hours. Nanorods of the hexagonal phase $NaEuF_4$ with a diameter of 20–30 nm and a length of 60–100 nm were obtained. An increase in the Eu^{3+} : NaF ratio from 1 : 4 to 1 : 10 led to the formation of a phase with a cubic fluorite-type structure (spheres ~200 nm in diameter) and the lattice parameter of 5.61 Å. Based on the phase diagram presented by Thoma *et al.*,[79] the composition $Na_5Eu_9F_{32}$ was assigned to this phase. In reality, the compound with this formula does not exist.[76] Based on the dependences of the lattice parameter of fluorite phases of variable composition in $NaF–LnF_3$ systems,[80] it can be concluded that nanoparticles have the composition $Na_{0.38}Eu_{0.62}F_{2.24}$. Chemical analysis is required to solve the problem.

Canadian researchers studied in detail precipitation of nanosized fluorides LaF_3, $LaF_3:Eu$ and $La_{0.45}Yb_{0.5}Er_{0.05}F_3$ and modifications of their surfaces.[12, 13, 81–83] A solution of rare-earth nitrates was mixed with a solution of sodium fluoride to yield LaF_3 : 5% LnF_3 nanoparticles and then fluorides were precipitated by adding ethanol. The particles were separated by centrifugation, washed with ethanol and dried *in vacuo*. The average particle size was ~20 nm.[13]

The $KY_{2+x}F_{7+3x}$ phase with variable composition ($0.5 < x < 1$) with a fluorite-type structure and a particle size of 17 nm was synthesised by mixing concentrated KF and $Y(NO_3)_3 \cdot 6H_2O$ solutions followed by stirring for 30 min, centrifugation and washing with deionised water.[84] Heating to 550–850 °C leads to ordering of the crystal lattice and the appearance of lines belonging to a superstructure in X-ray diffraction patterns.

Very important results on the morphology evolution of LaF_3 nanoparticles during its precipitation from $La(NO_3)_3$ and KF solutions (including the reaction at constant pH) were obtained.[85, 86] Successive transformations of amorphous hydroxyfluoride into crystalline LaF_3 nanoparticles of hexagonal shape, empty spheres with a diameter of several hundred nanometres consisting of agglomerates formed by small particles and the transformation of spheres into needles and ribbons were observed.

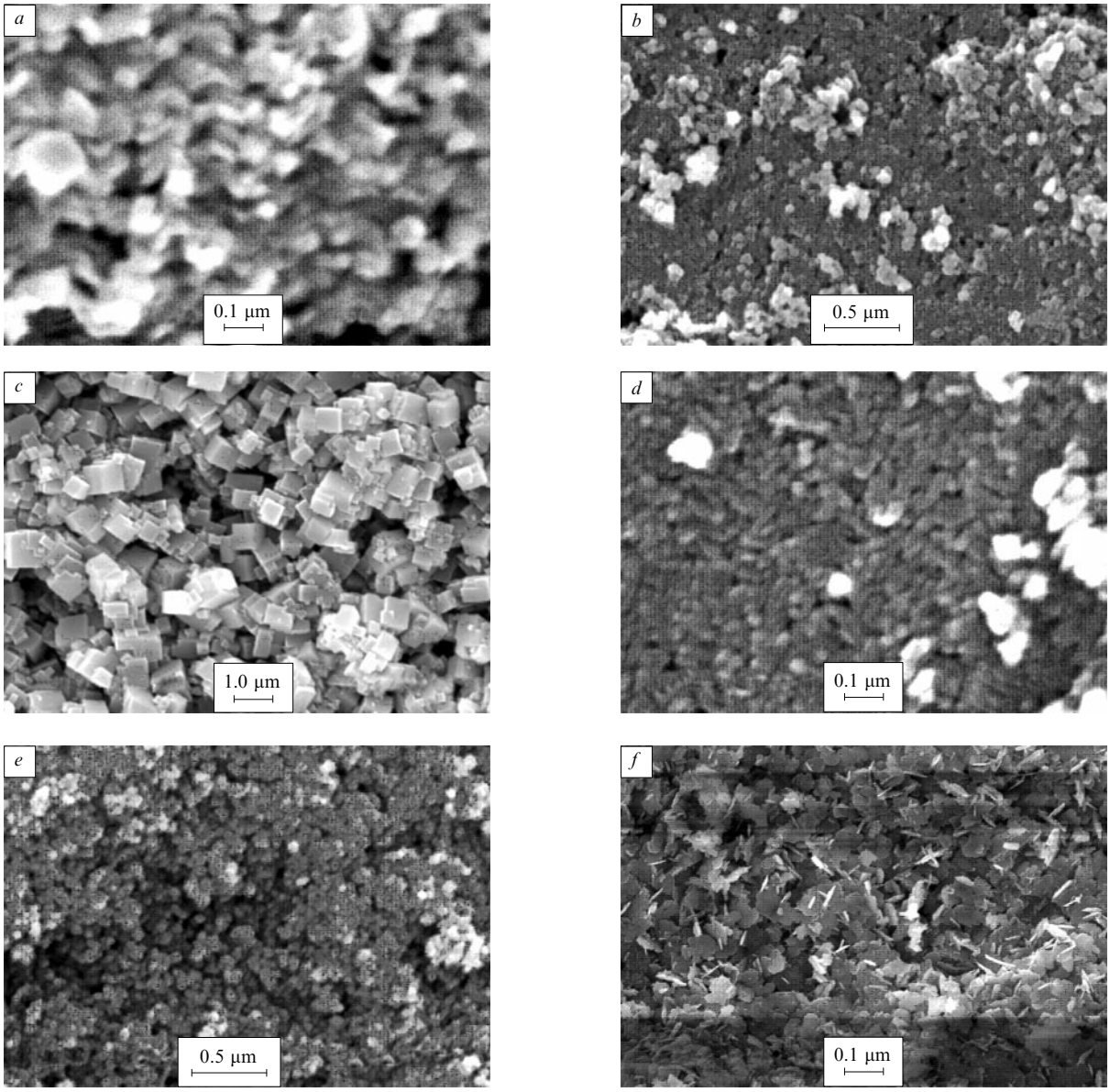


Figure 4. Electronic images of fluorides prepared by precipitation from aqueous nitrate solutions.
(*a*) $Ca_{0.9}Er_{0.1}F_{2.1}$ after precipitation by titration into hydrofluoric acid; (*b*) $Ca_{0.9}Er_{0.1}F_{2.1}$ after washing with ethanol; (*c*) $Ca_{0.9}Er_{0.1}F_{2.1}$ after drying at 150 °C; (*d*) $Ca_{1-x}Yb_xF_{2+x}$ after precipitation by titration with hydrofluoric acid; (*e*) $Sr_{1-x}Nd_xF_{2+x}$ after precipitation by titration with hydrofluoric acid, washing and prolonged drying at $\leqslant$100 °C; (*f*) BaF_2 after precipitation by titration with an ammonium fluoride solution.

Selected photomicrographs of fluoride particles, which we have synthesised ‡ by precipitation from aqueous solutions, are shown in Fig. 4.

Stabilisation of colloidal solutions of fluoride nanoparticles presents a special problem. The preparation of colloidal solutions of $NaYF_4$ (the particle size was 5–30 nm) was documented.[87] A procedure was developed [13] for dispersion of colloidal LaF_3 nanoparticles in solution with the use of citrate ligands adsorbed on the surface of nanoparticles.§

Crystallisation of nanoparticles from solutions can be performed under conditions of hydrothermal synthesis. This is used for the synthesis of many complex fluorides, for example, of $NaYF_4$;[88] $NH_4Er_3F_{10}$,[89] KMF_3 (M = Mn, Co, Ni, Zn or Mg);[90] K_2LnF_5, $KLnF_4$, KLn_2F_7, KLn_3F_{10};[91–93] $LiYF_4$, KYF_4 and $BaBeF_4$.[94] The particle size increases as the temperature of the synthesis and the reaction time are increased.

In some case, fluorides precipitated from solutions were subjected to additional mild (at a temperature lower than 180 °C) hydrothermal treatment. Nanocrystalline fluorides of La, Pr, Nd, Sm and Y were synthesised [95,96] from the oxides Ln_2O_3 (Ln = Y, La, Pr, Nd or Sm) dissolved in 10% nitric acid. A NH_4F solution was added to the nitrate solutions to obtain colloidal precipitates and a 10% KOH (or NaOH) solution was added to pH 4–5. Colloidal precipitates were stored in an autoclave at 80–180 °C for 12–24 h. The precipitates were filtered off, washed and dried in air at 80 °C. The resulting fullerene-like nanoparticles had a shape of empty spheres, their diameter increased from 10 to 30–50 nm as the temperature in the autoclave was increased from 120 to 180 °C.

‡ S V Kuznetsov, T T Basiev, V V Voronov, S V Lavrishchev, V V Osiko, E A Tkatchenko, P P Fedorov, I V Yarotskaya, in *Proceedings of the Second International Siberian Seminar INTERSIBFLUORINE-2006* (Tomsk: Institute of Inorganic Chemistry, 2006) p. 135.

§ See also F Wang, Y Zhang, X Fan, M Wang *J. Mater. Chem.* **16** 1031 (2006).

$LaF_3:Yb^{3+}, Er^{3+}$ nanoparticles were prepared by the hydrothermal synthesis.[97]

Nanoparticles can also be formed upon sonication (sonochemistry). The addition of an NaF alkaline solution to an acidic solution of rare-earth nitrates with intense sonication followed by hydrothermal treatment led to the formation of $YF_3:Ln^{3+}$ nanoparticles.[98]

The hydrothermal synthesis of nanoparticles of rare-earth oxofluorides was patented.[99,100]

Non-aqueous solvents can be used for the synthesis of fluorides to decrease the degree of hydration and remove hydroxyl impurities. Needle-like NH_4LnF_4 particles (Ln = Nd, Sm, Eu, Gd or Tb) with nanometre cross-section were prepared from methanolic solutions.[57] Nanorods with composition $PbBr_{2x}F_{2(1-x)}$ ($x = 0.15$, 0.3) were prepared from methanolic solutions of lead acetate, potassium fluoride and cetyltrimethylammonium bromide or potassium bromide.[101]

Particles with composition $KNiF_3$ as empty spheres with a diameter of 200–400 nm were synthesised by the solvothermic reaction in ethanol at 110 °C with the use of KF and $NiCl_2$ as the starting reagents. According to the results of transmission electron microscopy, these spheres consist of nanoparticles with the size of 10 nm (the wall thickness was 20–40 nm).[102]

Nanoparticles of CeF_3 with the size of 5–10 nm were synthesised from a solution of $CeCl_3$ and HF in ethylene glycol at 180 °C.[103] The nanoparticles were washed with ethanol, separated from the liquid phase by centrifugation and dried.

Synthesis from solution of metal acetates and alkoxides in non-aqueous solvents (isopropyl alcohol or methanol) by treatment with anhydrous hydrogen fluoride provides the basis for one of modifications of the sol–gel process (see below).

d. Precipitation from solutions in nanoreactors

The use of the so-called nanoreactors enables one to limit mechanically the sizes of the resulting particles. Solid porous templates, such as zeolites, gels or opals, can serve as nanoreactors.[49] Optical transmission of products is essential for their use in photonics.

Silica gel was also used.[49,104] Borosilicate glasses with the pore size of 4 nm pressed into pellets and Al_2O_3 ceramics with the pore size of up to 0.1 μm served as porous templates.[105] Porous membranes were placed between aqueous solutions of $Pb(NO_3)_2$ and NH_4F with concentrations of 0.1 mol litre^{-1}. The reaction produced PbF_2 nanoparticles in pores, both the equilibrium orthorhombic modification and the high-temperature cubic modification being obtained.

The reversed microemulsion method has gained wide acceptance in the synthesis of fluoride nanoparticles. This method has been developed in detail for other classes of compounds. The history of the problem was covered in the review.[2] Back in 1943, it was found [106,107] that certain ratios of water, an organic phase and two surfactants give quasihomogeneous mixtures called quaternary microemulsions. Long-chain organic molecules containing a hydrophilic head and a lipophilic tail (for example, cetyltrimethylammonium bromide, CTAB) are miscible with both hydrocarbons and water (Fig. 5*a*). Due to ion-dipole interactions, surfactants form spherical aggregates encapsulating water, the polar (ionic) ends of surfactant molecules being oriented inward (Fig. 5*b*). The orientation of molecules in microemulsions leads to minimisation of the surface tension thus providing stability, including thermodynamic stability, as opposed to usual macroemulsions. Such emulsions are called reversed emulsions because water in such emulsions is dispersed in an organic matrix.

It was suggested that quaternary reversed microemulsions were used for the preparation of colloidal non-charged particles.[108] The method consists of preparing two solutions of emulsions with required anions and cations, respectively, followed by mixing of these solutions to prepare the target compound (Fig. 5*c*–*e*). Emulsions with different volumes of an aqueous

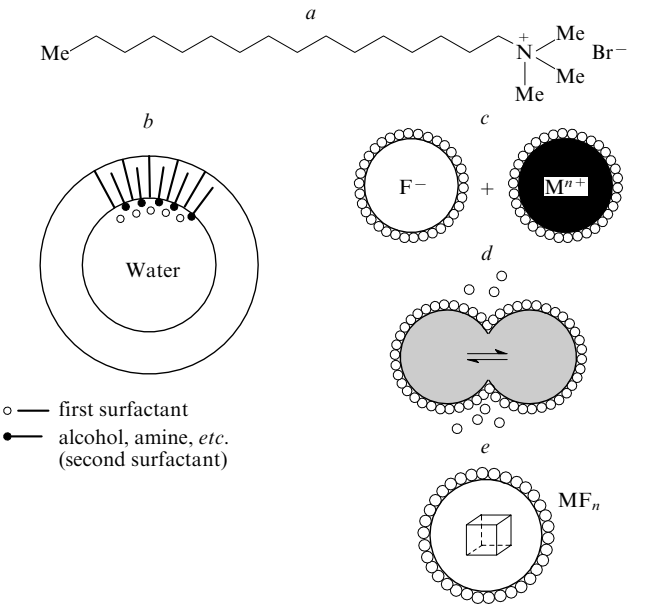


Figure 5. The CTAB molecule (*a*) and schemes of the structure of a microemulsion (*b*) and the synthesis of nanofluorides MF_n by the reverse a microemulsion method (*c*–*e*).

phase (a nanoreactor) can be prepared by varying the ratio of the aqueous and organic phases and the amount of a surfactant, which allows one to obtain nanoparticles of the desired size. The resulting particles are subjected to either coagulation (for example, by adding acetone) or centrifugation until a precipitate is formed, and the precipitate is washed, for example, with methanol. A classical microemulsion quaternary system has the following composition: n-butanol/CTAB, n-octanol/water. This approach is applicable to compounds poorly soluble in water ($\sim 10^{-5}$ mol litre^{-1}) and is used for the synthesis of fluoride nanoparticles. In some cases, ternary microemulsions, in which the second surfactant is absent, are used instead of quaternary microemulsions.

The synthesis of NH_4MnF_3 nanoparticles with sizes of 10–60 nm with the use of n-heptane/NH_4(AOT)/water microemulsions [AOT is bis(2-ethylhexyl)sulfosuccinic acid] and concentrated aqueous NH_4F and $Mn(OAc)_2$ solutions was documented.[109] An increase in the reaction time, a decrease in the salt concentration, an increase in the percentage of the aqueous phase and increase in temperature lead to enlargement of crystallites.

Fluoromanganates ($KMnF_3$ and $NaMnF_3$) exhibiting magnetic properties were synthesised [110] according to the reaction

$$MnCl_2 + KF \longrightarrow KMnF_3\downarrow + KCl \qquad (10)$$

with the use of the following microemulsion system: n-octane/CTAB, n-butanol/water. The particle size depends on the volume of nanoreactors. Particles of the same compounds with the size of 30 nm were synthesised by Carpenter [111] with the use of an emulsion system containing dioctyl sulfosuccinate, isooctane and water.

The synthesis of BaF_2 nanoparticles containing up to 65 mol.% NdF_3 was documented.[112] Emulsion systems consisted of cyclohexane, Igepal CO-520, ethanol and aqueous solutions of salts of the target cations and hydrofluoric acid. An increase in the concentration of the precursor leads to an increase in the size of the resulting crystallites. Powder X-ray diffraction study demonstrated that nanoparticles are heterogeneous and consisted virtually of pure BaF_2 and solid solutions $Ba_{1-x}Nd_xF_{2+x}$ with different concentrations. It was hypothesised that BaF_2 is repeat-

edly precipitated on the surface of nanoparticles enriched in neodymium. The resulting samples were tested for the presence of impurities. An IR spectroscopic study demonstrated that up to 3 mass % – 5 mass % of precursor ions, as well as hydroxyl groups, are present in samples prepared starting from nitrate and acetate salts. If precursors are readily soluble salts, the amount of impurities in samples is smaller.

The synthesis of BaF_2 nanoparticles and a solid solution $Ba_{1-x}Ce_xF_{2+x}$ ($x = 0.033$) with the use of an octan-2-ol/CTAB/water microemulsion system was documented.[113] It was found that the particle size decreases as the fraction of water in the system and the reaction time decrease. After washing of nanoparticles with ethanol, the final product contained traces of nitrate ions and hydroxyl groups (IR spectroscopic data).

The synthesis of CeF_3 nanoparticles from a polyisobutane – butanediimide/cyclohexane/water emulsion system was performed.[114] An increase in the percentage of water and the precursor concentration strongly influences the size and morphology of the resulting particles. The crystal structure was described as cubic face-centred, which does not correspond to the structure of bulk samples of CeF_3.

Nanoparticles of CeF_3 and the solid solution $Ce_{1-x}Lu_xF_3$ ($x \leqslant 0.5$) were synthesised by the microemulsion method.[115] The hexagonal structure typical of CeF_3 was found for all samples. The maximum luminescence intensity at ~ 325 nm is observed for $x = 0.3$.

An n-octane/CTAB, n-butanol/water microemulsion system was used in the synthesis of BaF_2 nanoparticles, including those activated with 6 mol.% europium and erbium.[116–118] It was found that only cubic nanoparticles grow until the critical size of the growing nanoparticle is smaller than the volume of the elementary reaction zone. As soon as the size becomes larger than this volume, the growth of dendrites begins. The edge lengths of cubic particles without dendrites were 100 – 200 nm. In the presence of dendrites (data from transmission electron microscopy), the aggregate size was 400 – 450 nm. Self-organisation of BaF_2 nanoparticles, which were synthesised by the reversed microemulsion method, giving rise apparently to dissipative structures was described.[119]

The use of microemulsions in the synthesis of particles of solid solutions of the general formula $K(Y,Ln)_{2+x}F_{7+3x}$ ($0.5 < x < 1$) with a size of 14 nm was documented.[84]

e. Variations of the sol – gel method

Crystallisation techniques used for the synthesis of bulk crystals in gels [120, 121] make it possible to decrease substantially the rate of chemical reactions due to an increase in the path length of the ion counter diffusion resulting in the formation of a new poorly soluble phase. This situation is ideal for the preparation of nanoparticles characterised by a low degree of agglomeration and investigation of the mechanism of their crystallisation. However, the output of this process is low, and other modifications of the sol – gel technology were used for the synthesis of fluoride nanoparticles.

According to one version, a porous homogeneous hydroxyl sol – gel is prepared and subjected to low-temperature treatment with a fluorinating agent giving rise to a highly dispersed amorphous powder, which becomes more compact on heating. This approach was developed for the synthesis of fluoride glasses.[39, 122, 123] A sol of nanocrystalline MgF_2 was synthesised by the reaction of hydrofluoric acid with the sol prepared from a methanolic solution of H_2O_2 and $Mg(OMe)_2$.[124]

In another version, a fluorinating agent (generally, trifluoroacetic acid) is directly used as one of the starting compounds along with metal acetates and alkoxides for the preparation of gels.[22, 27, 125 – 127]

$BaMgF_4$ doped with Eu^{2+} was synthesised from a solution of a mixture of barium, magnesium and europium acetates in isopropyl alcohol.[128] Trifluoroacetic acid and water were added to the solution to give a trifluoroacetate gel; its heating to 500 °C led to crystallisation of BaF_2 from the amorphous state (data from powder X-ray diffraction). At 550 – 600 °C, $BaMgF_4$ particles appeared.

An attempt was made to synthesise analogously KGd_2F_7.[129] Gadolinium and potassium acetates were dissolved in a stoichiometric ratio in isopropyl alcohol under argon in a Teflon reactor. Trifluoroacetic acid was added to the solution and the mixture was stirred for 3 h. Then a quartz substrate was coated with this solution and heated at 650 °C for 40 min under a stream of dry argon. The resulting product consisted of submicrometre-sized particles and contained oxygen as an admixture. Its composition corresponds to the formula $K_{0.31}Gd_{0.69}F_{1.84}O_{0.27}$. The monoclinic lattice parameters are similar to the lattice parameters of anhydrous KGd_2F_7.

In the third version of the sol – gel method, a silicate gel containing fluoride nanoparticles is prepared. Mixing of a silicate sol and a MgF_2 sol affords nanoparticles dispersed in an amorphous matrix. Heating results in a composite $MgF_2 - SiO_2$.[124] An improved modification of this process was patented.[130] Nanocrystals of LaF_3 (10 – 30 nm) in a silicate gel were synthesised by the sol – gel method starting from trifluoroacetic acid, lanthanum acetate, tetramethyl orthosilicate, methanol and dimethylformamide followed by heating of the gel to 300 °C. At 800 °C, pyrohydrolysis of LaF_3 started.[104] Glass ceramics can be prepared analogously.[131] For example, nanocrystallites of LaF_3 in transparent SiO_2-based glass ceramics were synthesised by the sol – gel method.[132]

A special modification of the sol – gel process was developed [17, 18, 20, 133, 134] with the aim of synthesising fluoride catalysts with highly developed surface. In the first step, solutions of metal alkoxides in a non-aqueous solvent (for example, aluminium isopropoxide in isopropyl alcohol) are treated with anhydrous hydrogen fluoride to yield an amorphous catalytically inactive solid as a precursor of the fluoride. The F : Al ratio in this precursor of AlF_3 was approximately equal to 2 : 1, the carbon content was 31%, and the specific surface area was 430 $m^2\ g^{-1}$ (Ref. 17). In the general form, the reaction equation is as follows:

$$Al(OR)_3 + x\,HF \longrightarrow AlF_x(OR)_{3-x} + x\,ROH \qquad (11)$$

($x = 0 – 3$); for aluminium isopropoxide existing as a tetramer, the equation is as follows:

$$Al[(\mu\text{-}OPr^i)_2Al(OPr^i)_2]_3 + 4x\,HF \longrightarrow 4\,AlF_x(OPr^i)_{3-x} + 4x\,Pr^iOH. \qquad (12)$$

Treatment of the products with a fluorinating reagent (CCl_2F_2) at 350 °C affords an amorphous AlF_3 powder with a specific surface area of 206 $m^2\ g^{-1}$ and the carbon content of 0.4 mass%, which is characterised by very high catalytic activity. Heating leads to crystallisation accompanied by an exothermic effect at 540 – 570 °C, which corresponds to the formation of α-AlF_3.

Magnesium fluoride with a specific surface area of 190 $m^2\ g^{-1}$ and mixed catalytically active fluorides with highly developed surface [$MgF_2 : FeF_3$ (Ref. 18) and $MgF_2 : CrF_3$ (Ref. 20)], in which magnesium fluoride serves as a sorbent (support), were synthesised analogously. The scheme of the process is shown in Fig. 6. It was hypothesised that the true sol – gel process occrus to give a three-dimensional random network analogous to networks of classical gels (in particular, of a silicate gel). Random binding of fluoroaluminate octahedra postulated in the fluoride gel corresponds to the network in fluoroaluminate glasses.

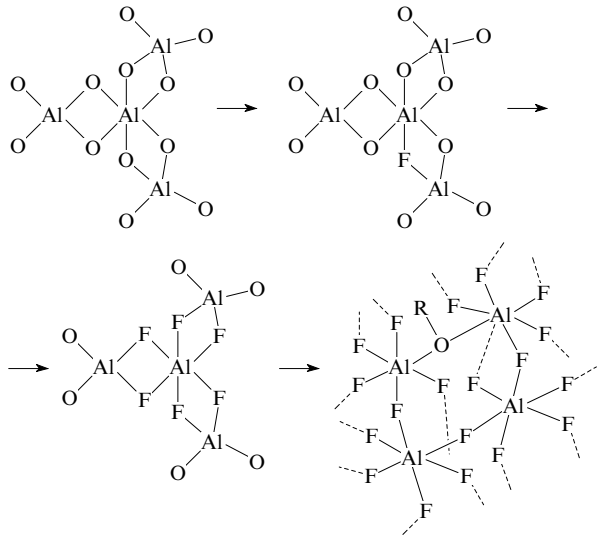


Figure 6. Scheme of the formation of a random network in different steps of the sol–gel process with the successive replacement of oxygen atoms by fluorine in bridging bonds.[134]

f. Miscellaneous methods of synthesis

Nanoparticles of potassium, barium and strontium fluorides and sodium chloride were prepared[6] by the flame synthesis. The corresponding precursor (metal 2-ethylhexanoate) was mixed with a stoichiometric amount of fluoro- or chlorobenzene, and the mixture was nebulised in a methane–oxygen flame. The resulting product was collected on a heated filter to prevent water condensation. The particle size of CaF_2 was 20 nm.

UF_5 nanoparticles were synthesised by laser photolysis of gaseous UF_6 in a supersonic nozzle reactor for isotope separation.[135–137]

A study[138] on the synthesis of single-crystalline PbF_2 nanoparticles by selective chemical dissolution of bulk nanocomposite oxyfluoride glass ceramics is of interest. Impurity-free lead fluoride nanoparticles with the size of 15 nm doped with Eu^{3+} ions show intense fluorescence (green and blue) after IR excitation.

Fluoride nanoparticles can be prepared by gas-phase fluorination of dispersed systems.

IV. One-dimensional nanoobjects

Unique physical properties of one-dimensional (or 1D) nanoobjects and the possibility of producing functional materials based on these nanoobjects have attracted considerable attention.

Whisker crystals characterised by exceptional mechanical properties are typical 1D objects.[139, 140] The main mechanism for their growth is the so-called vapour–liquid–crystal mechanism according to which growth occurs from the vapour phase through a melt drop. The diameter of whisker crystals is determined by the size of the starting drop and is generally of a micrometre size. A decrease in the drop diameter leads to a decrease in the growth rate (due to a change in the vapour pressure over the drop). Nevertheless, it is possible to grow such thin whiskers. Whisker crystals were prepared from the vapour phase for such fluorides as LiF, NaF (Refs 121 and 139) (Fig. 7) and CdF_2.[141]

Another procedure for the preparation of 1D nanoobjects is based on crystallisation from solution.[139] Nanorods of the hexagonal phase $NaEuF_4$ 20–30 nm in diameter and 60–100 nm in length were prepared from aqueous solutions of europium nitrate and sodium fluoride.[78] Whisker crystals of BaF_2 oriented along the [111] direction with a length of 50 μm and a size ratio of 1000 : 1 were synthesised by the hydrothermal method with the use of a microemulsion.[142] The crystal thickness was determined by the drop size.

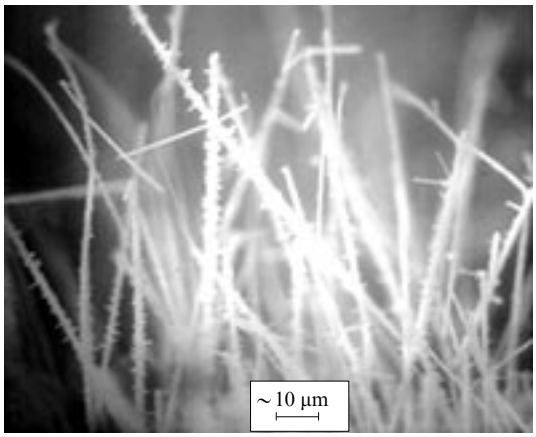


Figure 7. Whisker NaF crystals grown from a vapour phase with the use of BaFCl as a transport reagent.

Precipitation of compounds $PbBr_xF_{2-x}$ ($x \leqslant 0.3$) from methanolic solutions afforded needle-like nanoparticles 30–50 nm in diameter and 500–1000 nm in length;[57] NH_4LnF_4 particles (Ln = Nd, Sm, Eu, Gd or Tb) were synthesised by solvothermic treatment of the precipitate at 150 °C.[101] Thermolysis of the fluoroammonium complexes NH_4LnF_4 produced rare-earth trifluorides. The shape memory effect, *i.e.*, the retention of the particle shape, was observed. The resulting 1D nanoobjects were characterised by high concentration of structural defects.

One-dimensional nanoobjects correspond to one of steps of evolution of LaF_3 nanoparticles as the F : La ratio increases during titration in an aqueous solution.[86]

V. Two-dimensional nanoobjects

Films are typical two-dimensional (2D) nanoobjects. Islet films, which represent nanoparticle ensembles on a substrate, are natural and one of the simplest elements of the nanocrystalline architecture.

The formation of fluoride films was studied in detail. In addition to fundamental problems, there are several practical applications due to which these objects have attracted interest: antireflection coatings,[143–146] epitaxial dielectric films on semiconductors[147] and luminescent coatings.[129, 148–152]

The lattice parameters of calcium and cadmium fluorides (a = 5.463 and 5.388 Å, respectively) are similar to the silicon lattice parameter (a = 5.4305 Å). Layers, that are similar in the characteristic geometric sizes to the Si(111), Ge(111) and GaAs(111) planes are present in the structures of rare-earth trifluorides (in particular, [001] in the tysonite structure). This fact has stimulated interest in the preparation and investigation of the corresponding epitaxial layers.[147, 153, 154]

The cubic lattice parameter can be varied in a wide range (from 5.388 to 6.20 Å), and coatings for lead chalcogenides can be adjusted based on this parameter with the use of the solid solutions $Ca_{1-x}Sr_xF_2$ and $Sr_{1-x}Ba_xF_2$ as well as by the introduction of rare-earth metals into the fluorite structure (giving rise to the solid solutions $M_{1-x}Ln_xF_{2+x}$).[149, 155]

However, the difference in the thermal expansion coefficients, which are 3–7 times larger for fluorides than for semiconductors, is a serious problem.

A small difference in the lattice parameters of deposited layers makes it possible to construct heterostructures.[156] Dielectric fluoride layers are used for the construction of more complex structures, for example, of metal–insulator–semiconductor systems.[157]

In addition to molecular beam epitaxy,[148, 149, 151] spray coating,[145, 158] chemical vapour phase deposition,[53, 55] magnetron spraying,[159] deposition of fluoride films by soft chemistry

methods has been developed in recent years (Refs 125, 128, 160–163 as well as ¶).

VI. Fluoride nanocomposites

1. Glass ceramics

In recent years, the properties and procedures for the preparation of glass ceramics, such as the generation of a micro- or nanodispersed crystalline phase in a glass matrix, have been extensively studied.[164] As a rule, such materials are prepared by crystallisation of glasses, *i.e.*, by thermal treatment at near-crystallisation temperature. One of the aims is to prepare transparent glass ceramics for nanophotonics.[165–167] Such materials have a series of novel properties and are free from many drawbacks of glasses and single-crystalline materials. These materials are processable, they are suitable for the preparation of fibres characterised by a high capacity for activating ions and the isotropicity and homogeneity of properties and activator concentrations.

In practice, there is often a need for functional materials in which the distribution coefficients of activator ions between the matrix and nanoparticles are substantially different. The transfer of an activating additive in the crystalline environment leads to narrowing of luminescence linewidths and an increase in luminescence intensity compared to the intensity of the analogous luminescence of glasses. In particular, this can be achieved by preparing fluoride nanoparticles in a silicate or aluminosilicate matrix.

LaF_3,[168–172] PbF_2 (Refs 173 and 174 as well as †), $Pb_{1-x}Cd_xF_2$ (Refs 165–167 and 175–177) and CaF_2 (Ref. 178) can serve as fluoride particles accumulating rare-earth ions. In some cases, nanoparticles of solid solutions $M_{1-x}Ln_xF_{2+x}$ at high concentrations were obtained.

Crystallisation of the glass with composition $16.5\,Al_2O_3 \cdot 1.6\,AlF_3 \cdot 12.7\,LaF_3 \cdot 4.3\,Na_2CO_3 \cdot 64.9\,SiO_2$ afforded the LaF_3 phase where rare-earth elements were incorporated in a different proportions: Er^{3+}, 2%–3% of the total amount of the introduced erbium fluoride; Pr^{3+}, up to 70%.[169]

The preparation of a transparent glass-crystalline material based on the glass with composition $30\,SiO_2 \cdot 15\,AlO_{3/2} \cdot 29\,CdF_2 \cdot 17\,PbF_2 \cdot 5\,ZnF_2 \cdot 4\,YF_3$ was documented.[166, 167] The glass transition temperature and the crystallisation temperature of the starting glass are 395 and 475 °C, respectively. Thermal treatment with the aim of preparing glass ceramics was carried out in the temperature range of 440–470 °C for 30–60 min. The crystallite size was 6–8 nm.

Glass ceramics with similar composition, $30\,SiO_2 \cdot 15\,AlO_{1.5} \cdot 28\,PbF_2 \cdot 22\,CdF_2 \cdot (4.8-y)\,GdF_3 \cdot 0.1\,NdF_3 \cdot y\,YbF_3 \cdot 0.1\,TmF_3$ (y = 0, 0.1, 0.2, 0.5, 1.0, 2.0, 3.0, 4.0 and 4.8), were prepared.[179] The crystallite sizes in this system are virtually independent of the annealing time (Fig. 8 *a*). Therefore, thermal treatment did not lead to growth of fluoride particles, which were already present in the glass.

In addition to crystallisation of cast glasses, sol–gel methods are used.[131, 132, 180] The glass ceramic with composition $0.1\,ErF_3 \cdot 0.1\,YbF_3 \cdot 5\,LaF_3 \cdot 94.8\,SiO_2$ was prepared by Fujihara's method.[132] Tetraethoxysilane (TEOS), which was dissolved in an equimolar amount of ethanol, was hydrolysed with water in the presence of acetic acid as the catalyst. The TEOS : H_2O : AcOH ratio was 1 : 10 : 0.5. Rare-earth acetates were dissolved in trifluoroacetic acid (M^{3+} : F^- = 1 : 10). A small amount of water was added to accelerate dissolution. The trifluoroacetate solution was slowly stirred with silica sol. The gel formation occurred at room temperature for two weeks. Drying was performed at 40–70 °C for one week. The dry gel was heated to 1000°C in air at a rate of 75 K h^{-1}, after which the sample became more compact and transparent glass ceramics involving fluoride nanoparticles was obtained. Lanthanum fluoride nanoparticles doped with erbium were dispersed as a colloidal solution in a silica sol that is formed upon hydrolysis of tetraethoxysilane. The disperse system was coated onto a substrate to prepare thin films.[180]

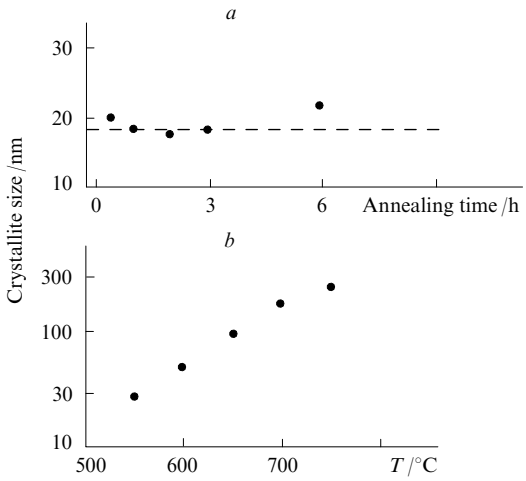


Figure 8. Plots of the crystallite size *vs* the parameters of thermal treatment.
(*a*) The particle size of $Pb_{1-x}Cd_xF_2$ in the $30\,SiO_2 \cdot 15\,AlO_{1.5} \cdot 28\,PbF_2 \cdot 22\,CdF_2 \cdot (4.8-y)\,GdF_3 \cdot 0.1\,NdF_3 \cdot y\,YbF_3 \cdot 0.1\,TmF_3$ glass *vs* the annealing time;[179] (*b*) the particle size of LaF_3 in the $53\,SiO_2 \cdot 11\,Na_2O \cdot 27\,Al_2O_3 \cdot Al_2F_6 \cdot 7\,La_2F_6 \cdot 0.07\,Er_2F_6$ glass *vs* the temperature of thermal treatment for 12 h.[173]

According to the commonly accepted Gleiter concept, glasses (as opposed to composite materials) are considered as uniform homogeneous media.[181] However, this concept is doubtful as referred to nanomaterials. Not only short-range but also medium-range order regions tens of ångströms in size were found in glasses by different methods. A crystallite model of glasses, which was proposed by Lebedev more than 80 years ago [182] and was considered as an antithesis to the Zachariasen–Warren theory of continuous random networks,[183–185] has been confirmed and defined more specifically in recent years (due to the use of modern methods of investigation),[186–188] including the model of strained mixed clusters [189] (Fig. 9). Therefore, contrary to the opinion of Gleiter,[181] in some cases glasses can be considered as true nanocomposites where nanometre-size crystalline regions (they can have different compositions and structures) are surrounded by an amorphous strained defect shell. This is also true for fluoride glasses, which are promising materials for optical information transmission. A vast diversity of fluoride glasses includes the following main classes: fluorozirconate, fluorohafnate, fluoroaluminate, fluoroindate and fluoroberyllate glasses.[190–194]

In the light of the above, the crystallisation process can be considered as either an increase in the size of crystallites, which are already present in the glass, or as the appearance and growth of crystallites the structures of which differ from those present in the glass. Therefore, in some cases, structural difference between glasses and glass ceramics is rather quantitative than qualitative in essence.

The crystallisation processes of fluoride glasses, including those giving rise to transparent glass ceramics, were considered.[195–200] It was shown [201] that the optical transmission retained upon crystallisation of 90% of a fluorozirconate glass.

The plots of the crystallite size *vs*. the parameters of thermal treatment of oxofluoride glasses shown in Fig. 8 illustrate two different situations: (1) thermal treatment does not lead to growth of fluoride particles that are already present in the glass; (2) a rise

¶ B-Ch Hong, K Kawano *J. Alloys Compd.* **408–412** 898 (2006); P Jia, J Lin, M Yu *J. Lumin.* **122–123** 134 (2007).
† G Dantelle, M Mortier, D Vivien, G Patriarche *Opt. Mater. (Amsterdam)* **28** 638 (2006).

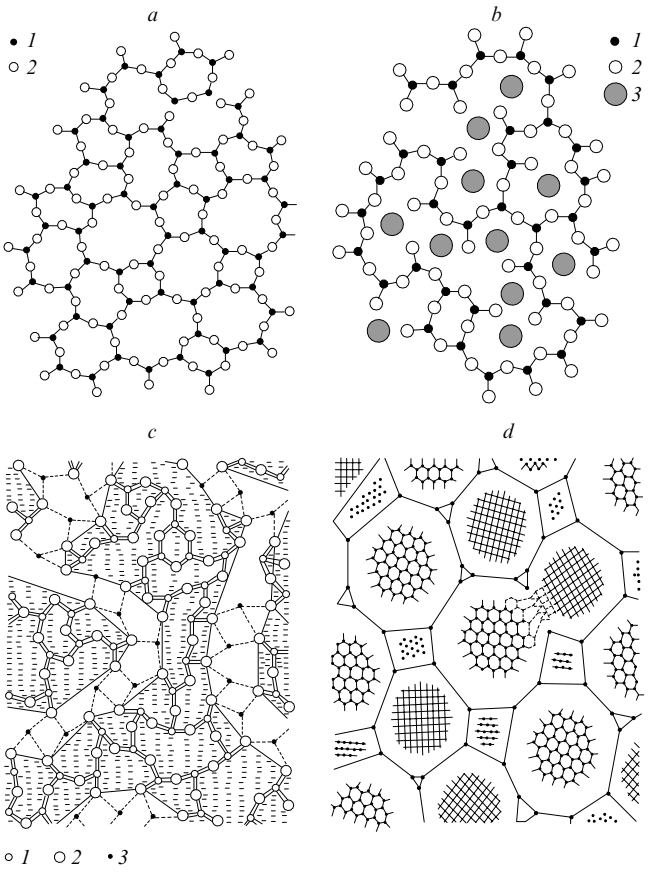


Figure 9. Models of glass structures.
(*a*) The Zachariasen model,[183] (*b*) the Warren model,[184, 185] (*c*) the Greaves model,[187] (*d*) the Goodman model (the model of strained mixed clusters).[189]
(*1*) Network-forming atoms, (*2*) bridging atoms, (*3*) network-modifying ions.

of the temperature leads to an increase in the particle size. In the latter case, glass ceramics with a particle size smaller than 60 nm (calculated from the line broadening in X-ray diffraction patterns) retain optical transmission.

The question of whether it is correct to consider glasses as nancomposites requires additional studies, including the use of atomic force [202] and transmission electron microscopy.

2. Single crystals of heterovalent solid solutions

Association of point defects in crystals gives rise to various complex defects the size of which together with the relaxation region of the matrix is equal to several unit cells, *i.e.*, corresponds to nanoobjects. On the whole, crystals containing defects at rather high concentration can be considered as nanocomposites (Fig. 10).

For fluoride systems, the solid solutions $M_{1-x}Ln_xF_{2+x}$ with a fluorite structure formed in MF_2-LnF_3 systems (M = Ca, Sr, Ba, Cd or Pb; Ln = La–Lu, Y or Sc) are typical examples of such nanocomposites.[204] Phase equilibria in these systems were studied in detail.[68, 155] The width of the solid solution regions reaches 50 mol.% ($x \leqslant 0.5$). At lower temperatures, solid solutions are thermodynamically unstable and either decompose or undergo ordering. However, these processes are hindered and single crystals grown from a melt retain optical transmission for decades.

The formation of such solid solutions is a typical example of heterovalent isomorphism with a variable number of atoms per unit cell.[205] Cations have different charges. Hence, the insertion of additional fluoride ions into the lattice of dilute solid solutions is necessary for electrostatic compensation (Goldschmidt's scheme)

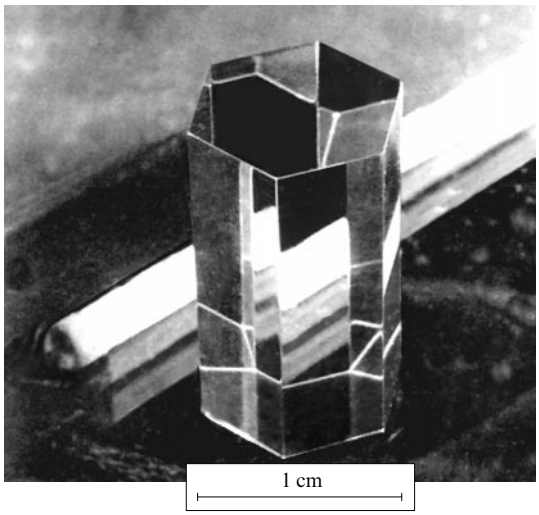


Figure 10. Nanocomposite as an artificially facetted single crystal of the solid solution $Sr_{0.69}La_{0.31}F_{3.31}$ corresponding to the maximum in melting curves of the solid solution with a fluorite structure in the SrF_2-LaF_3 system.[203]
Most refractory inorganic fluoride (T_m = 1570 °C).

$$M^{2+} \longrightarrow Ln^{3+} + F^-_{int}\,. \qquad (13)$$

Thus, there are two types of point defects in the fluorite lattice. Electrostatic interactions between these defects lead to their association to form dipoles ($Ln^{3+}-F_{int}$), which can have different crystallographic orientations. An increase in the concentration of rare-earth fluorides leads to further association of dipoles to form $(Ln^{3+}-F_{int})_2$ dimers and more complex associates (clusters).[206, 207] More than two dozens of cluster models were proposed based on data from various experiments and calculations.[204, 208, 209]

In solid solutions, the presence of Ln_6F_{37} clusters (Fig. 11) was reliably established.[210, 211] In these clusters, the coordination polyhedra of rare-earth metals are tetragonal antiprisms. An additional anion occupies the cuboctahedral cavity in the centre of the cluster. The existence of such clusters was revealed, in particular, by X-ray diffraction study of ordered fluorite-like phases in these systems. Such clusters are naturally incorporated into the fluorite lattice (see Fig. 11). Since the geometric sizes of associates differ from the size of the matrix lattice regions, which are replaced by these associates, the corresponding composites have local internal strains and deformations. The charge of the cluster differs from the charge of the fragment of the fluorite lattice. Hence, the formation of clusters is accompanied by elimination of an equal amount of additional anions into the matrix according to the equation

$$(M_6F_{32})^{20-} \longrightarrow (Ln_6F_{37})^{19-} + F^-_{int}\,. \qquad (14)$$

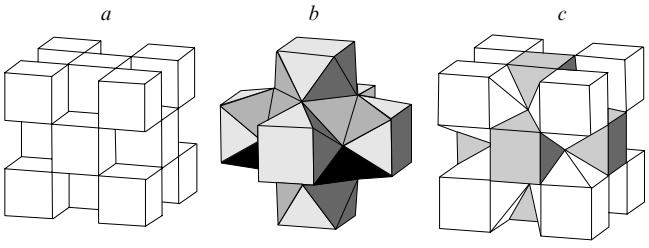


Figure 11. Fragment of the fluorite lattice (*a*), the Ln_6F_{37} cluster (*b*) and the Ln_6F_{37} cluster incorporated into the fluorite lattice (*c*).

Both an increase in the concentration of charge carriers and the presence of a deformed zone in the cluster shell lead to a sharp increase in the ionic conductivity.[212,213]

The formation of the solid solutions $M_{1-x}Ln_xF_{2+x}$ corresponds to the so-called block isomorphism. In this case, the long-range order in the packing of cations is retained, although the anion sublattice undergoes very strong local deformations.

The concentration of clusters increases with an increase in concentration of solid solutions. In the range of 6 mol.% – 8 mol.%, percolation occurs, *i.e.*, clusters get in contact with each other to form superclusters in which rare-earth elements are accumulated. The sizes of such superclusters can be as large as several micrometres.

The scheme of successive defect association in the fluorite structure is shown in Fig. 12. The concentration boundaries of the regions vary with temperature and depend on the chemical composition of the systems. The concentration range corresponding to individual clusters containing several rare-earth ions mainly belongs to the region of nanomaterials.

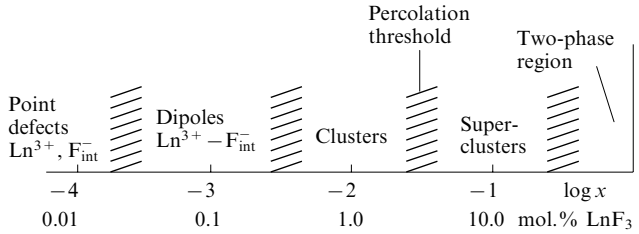


Figure 12. Regions of defect association in the solid solutions $M_{1-x}Ln_xF_{2+x}$ with a fluorite structure.

The structures of clusters in the solid solutions $M_{1-x}Ln_xF_{2+x}$ radically differ from the structures of rare-earth fluorides. Therefore, clusters cannot serve as nuclei of the LnF_3 phase. It is this fact that is responsible for stability of solid solutions against decomposition and the possibility of their use as photonic materials.

An analogous defect structure (poorly studied) is also typical of heterovalent solid solutions having a fluorite structure in the $MF_2 - XF_4$ (X = Zr, Hf, U or Th), $NaF - LnF_3$ and, to a lesser degree, $KF - LnF_3$ systems, as well as of phases with variable composition with a tysonite structure formed in the $MF_2 - LnF_3$ systems. There is also high similarity with fianites, which are solid solutions with a fluorite structure in the $Ln_2O_3 - (Zr,Hf)O_2$ systems.[206] Coherent submicrometre-size zones of the second phase are well known in metal alloys.

The term 'antiglass' was introduced [214] for the description of crystalline disordered phases characterised by essential local disorder in the presence of a long-range order (in usual glasses, the long-range order is absent, but they have a short- and medium-range order). The heterovalent solid solutions under consideration are typical antiglasses. The similarity of the physical properties of glasses and antiglasses is an example of the principle of equivalence of disorder sources proposed by Tretyakov.[215]

Taking into account the difference in principle between glasses (chaos with islets of order) and antiglasses (order with islets of chaos), antiglasses cannot be considered as an intermediate between crystals and glasses. It is more probable that antiglasses are antipodes of glasses. This main difference leads to a series of additional essential differences. Since solid solutions (antiglasses) are highly defect, they are characterised by a low entropy of melting and, correspondingly, have a low activation barrier to nucleation, and their melts solidify virtually without supercooling. To the contrary, glass-forming melts are characterised by strong supercooling. The appearance of antiglasses as strongly disordered crystalline phases with variable composition, the presence of clusters (defects) and the absence of supercooling are factors limiting the glass formation.

Glasses [for example, $ZrF_4 - BaF_2 - LaF_3 - AlF_3 - NaF$ (ZBLAN)] and antiglasses [for example, the solid solutions $Ba_{1-x}Ln_xF_{2+x}$ (Ln are rare-earth metals, $x \leqslant 0.5$) with a fluorite structure] have the following similar features:

— nanoheterogeneity, the cluster (crystallite) character of the structure;

— a high degree of disorder, high entropy;

— broad multicentre luminescence spectra, broadening, which does not disappear at lower temperatures;

— abnormal low-temperature thermal conductivity, the absence of maxima in the temperature dependence of thermal conductivity;

— fragility, the absence of cleavage;

— high ionic conductivity, the absence of a conductivity jump on melting;

— thermodynamic instability under standard conditions; an increase in the cooling rate expands the region of existence;

— variable chemical composition and high isomorphic capacity;

— dependence of physical properties (density, refraction index and conductivity) on the conditions of thermal treatment;

— characteristic features of vibrational spectra;

— percolation phenomena;

— polyfunctionality of materials based on these substances;

and the following differences:[205]

glasses are characterised by the presence of only a short- and medium-range order, a network structure, fusible composites, high entropy of melting, strong supercooling of melts, which depends on the cooling rate; antiglasses are characterised by a long-range order, a framework structure, refractory, maxima in the melting curves, slight supercooling of melts.[216]

3. Eutectic and eutectoid nanocomposites

Let us consider the possibility of preparing nanocrystalline composites by eutectic crystallisation. Steady-state crystallisation can afford rather ordered plate- or rod-like structures (the transition of one type into another is determined by the volume fraction of the crystallising phases).[217] An electronic image of the $LiF - LiCdF_4$ eutectic system with a fibre diameter of ~ 1 μm is shown in Fig. 13.[218]

For steady-state eutectic crystallisation, the following formula is true

$$\lambda^2 R = \text{const},$$

where λ is the characteristic linear size (for example, the rod diameter) and R is the crystallisation rate. Therefore, to decrease

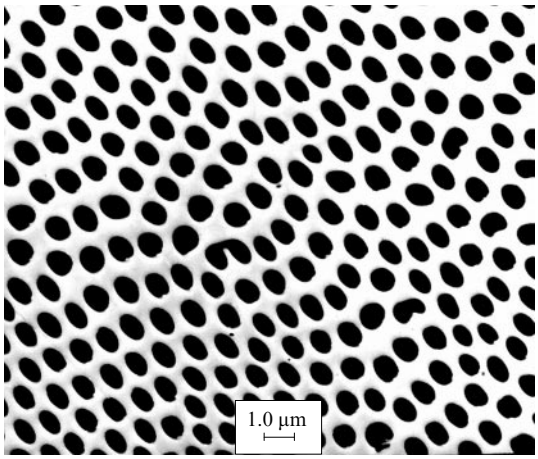


Figure 13. Electronic image of the eutectic composite $LiF - LiGdF_4$. Directed crystallisation at a rate of 10 mm h^{-1}, the temperature gradient was 70 K min^{-1}.

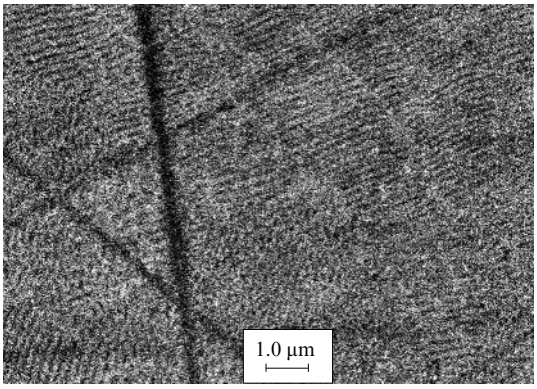


Figure 14. Image of the product of eutectoid decomposition of a solid solution in the BaF_2-CaF_2 system.[219]
Cooling at a rate of 100 K min^{-1}; straight dark lines correspond to scratches on the surface.

the rod diameter by a factor of 10, it is necessary to increase the rate by a factor of 100, which is difficult to perform technically for a steady-state process.

Eutectoid composites hold more promise. The microstructure of an alloy after eutectoid decomposition in a system consisting of calcium and barium fluorides is shown in Fig. 14. In this system, three phases having fluorite structures (solid solutions based on the components and an intermediate high-temperature phase) exist in equilibrium at 870 °C.[219] The sample is characterised by high ionic conductivity comparable with the conductivity of a specially formed composite prepared by successive deposition of nanolayers of calcium and barium fluorides.[220]

4. Oxide nanoparticles in fluoride matrices

Fluoride matrices are used for the insertion of nanoparticles with another chemical composition. For example, ZnO and $ZnGa_2O_4$ nanoparticles dispersed in MgF_2 or LaF_3 films were prepared by the sol–gel method.[221,222]

It is known that dispersion in an ionic matrix, including a fluoride matrix, of nanoparticles of dielectric materials, such as SiO_2 and Al_2O_3, causes an increase in ionic conductivity. This approach is known under the name 'heterogeneous doping'. The maximum conductivity is observed for a certain volume fraction of dispersed submicrometre-size particles. The theoretical aspects of heterogeneous doping were considered in the publications.[223–225] A substantial increase in the fluoride-ionic conductivity was observed in such heterogeneous systems as $CaF_2:Al_2O_3$, $BaF_2:Al_2O_3$,[226] $Ca_{0.995}Na_{0.005}F_{1.995}:CeO_{2-x}$ and $Ca_{0.992}Y_{0.008}F_{2.008}:CeO_{2-x}$.[227]

5. Other fluoride nanomaterials

In addition to inorganic fluorides, other compounds also belong to nanocrystalline materials. Evidently, crystalline fluoroorganic polymers,[228] like usual polymers, are nanoparticles (with an ordered arrangement of molecules), which are present in a matrix with a lesser degree of order, in a wide temperature range. These materials are analogues of glass ceramics.

Ultradispersed polytetrafluoroethylene (UDPTFE) powders were synthesised.[229] The technology of the preparation of this material is based on nucleation and condensation of gaseous products of thermal decomposition of industrial polytetrafluoroethylene (Fluoroplast-4). The sizes of particles formed in the gas medium are in the range of 25–50 nm.[229,230] Particles of an UDPTFE powder, the sizes of which vary from 100 to 1200 nm (the average size is 550 nm), consist of nanoblocks. A photomicrograph of an individual particle is shown in Fig. 15. The particles consist of blocks up to 100 nm in size. The blocks are held together by low-molecular-weight polytetrafluoroethylene

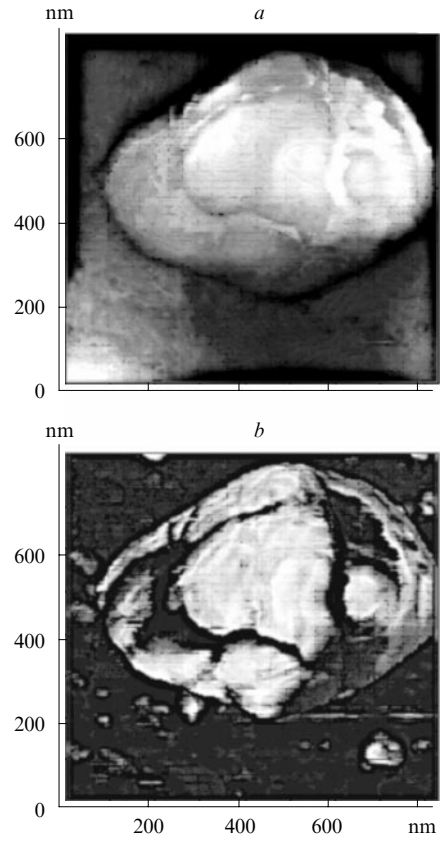


Figure 15. Images of a nanoparticle of ultradispersed polytetrafluoroethylene taken with the use of an atomic force microscope (courtesy of V M Buznik).
(*a*, *b*) Different measurement modes.

(PTFE), the structure and properties of which differ from those of the usual high-molecular-weight compound. Some particles are coated by this material. Low-molecular-weight PTFE is characterised by solubility in some solvents and supercritical carbon dioxide, which made it possible to prepare 2–4 nm thick polymeric coatings.[230]

A family of new nanomaterials, including magnetic materials, was synthesised by deposition of metal nanoparticles (Fe, Co, Ni, Cu or Pd) on the surface of ultradispersed PTFE granules. Deposition is accompanied by a chemical reaction. In some cases, nanoparticles have a complex composition. Defluorination of PTFE giving rise to a fluoride interlayer and a carbide layer was observed.[230–232] The structural model of an iron nanoparticle on the surface of an UDPTFE nanogranule is shown in Fig. 16.

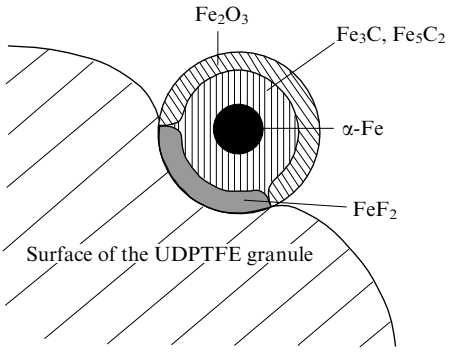


Figure 16. Structural model of an iron nanoparticle on the surface of an ultradispersed polytetrafluoroethylene nanogranule.[232]

VII. Nanotechnology and nanoarchitecture

As a rule, the synthesis of nanoparticles is merely the first step of the construction of materials. Fluoride nanoparticles are used in intermediate steps and for the construction of more complex structures of functional importance, *i.e.*, in the design of nanoobjects.

It was demonstrated [158] that decomposition of a CoF_2 film in a transmission electron microscope afforded cobalt nanoparticles with a size of 5–10 nm.

The introduction of YF_3 nanoparticles into a shell of polyelectrolyte multilayer capsules was found to improve their mechanical characteristics.[233] The scheme of this multistep process is shown in Fig. 17.

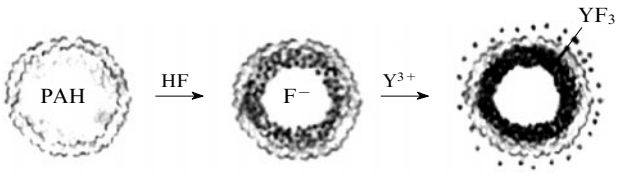


Figure 17. Scheme of the modification of polyelectrolyte capsules with yttrium fluoride nanoparticles.[233]
PAH is poly(allylamine hydrochloride).

One of operations in nanotechnology is coating of nanoparticles. Taking into account the luminescence properties of lanthanide compounds, interactions between active metal ions and OH^- ions, which are efficient luminescence quenchers, present a serious problem. The surface of nanoparticles of fluorides $Gd_{0.9}Er_{0.1}F_3$, which are present in a porous SiO_2 matrix, was coated with Gd_2O_3.[49] The suspension was placed in an aqueous solution containing Gd^{3+} and urotropine. Heating at 80 °C for 2 h led to deposition of a $Gd(OH)_3$ layer. Upon further heating to 500 °C, the hydroxide coating is transformed into the oxide coating. Decomposition of europium trifluoroacetate in a trioctylphosphine oxide (TOPO) melt afforded EuF_3 nanoparticles coated with TOPO, which prevents pyrohydrolysis and leads to the efficient energy transfer of europium radiation outwards.[51]

A more complicated nanotechnological process was employed [13] for the preparation of luminescent silica films containing LaF_3 nanoparticles doped with Er^{3+}, Nd^{3+} and Ho^{3+} (5% each) by the sol–gel method. The authors solved two problems: insulation of luminescent ions against OH groups (for this purpose, nanoparticles were coated with undoped LaF_3) and dispersion of colloidal nanoparticles in solution with the aim of their homogeneous inclusion into the sol–gel matrix (for this purpose, citrate ions adsorbed on the surface of nanoparticles were used). The following operations were performed successively: precipitation of nanoparticle nuclei, their coating, stabilisation in a colloidal solution, introduction of particles into a gel and film formation.

Studies on the synthesis of hybrid organic/inorganic systems based on fluoride nanoparticles were started (see, for example, Refs 25, 82, 234 and 235).

Coating of multilayer carbon nanotubes by EuF_3 and TbF_3 nanoparticles using intermediate hydrophobic interactions between the surface of carbon nanotubes and sodium dodecyl sulfate was documented.[236] The nanoparticle size was at most 10 nm.

VIII. Conclusion

In recent years, extensive studies in the field of nanotechnology of fluorides have been performed. However, it is obvious that these investigations are in their infancy and will be further developed, in particular, with the use of methods for the synthesis of nanoparticles (the aerosol method, thermolysis of fluoroammonium salts, *etc.*).

Further investigations of the influence of the dispersity on hydrolysis of fluorides and particularly studies of the first step, *viz.*, adsorption of water and other substances on the surface of fluoride particles, as well as the development of procedures for the preparation of protective coatings on the surface of fluoride nanoparticles, are required. Taking into account the similar sizes of the F^- and OH^- ions, it can be assumed that in many cases, where fluoride nanoparticles are synthesised from an aqueous solution or in air, these particles would contain a particular fraction of OH groups, which increases as the surface is approached (*i.e.*, nanoparticles are hydroxofluorides). According to the results of chemical analysis, the oxygen content increases with increasing amount of rare-earth metals in single crystals prepared by the hydrothermal method. The lattice parameters and the phase transition temperatures are in satisfactory agreement with the corresponding parameters of samples synthesised under anhydrous conditions. The available data (see, for example, Refs 11, 14 and 75) demonstrate that the degree of hydrolysis in the synthesis of nanoparticles increases when potassium is used instead of sodium, which is obvious taking into account substantially higher hygroscopicity of KF compared to NaF. In the case of precipitation of sodium–rare-earth element compounds, OH^- ions are virtually absent. For potassium compounds, substantial hydrolysis is observed. It should be noted that according to earlier data (see Refs 69, 70 anf 72), the degree of hydration in the case of precipitation with sodium fluoride and potassium fluoride from aqueous solutions of rare-earth salts of cubic double fluorides $M_{0.5-x}Ln_{0.5+x}F_{2+2x}\cdot n\,H_2O$ ($x = 0.05-0.17$) is smaller for M = Na ($n = 0.2-0.5$) than for M = K ($n = 1-3$).

It seems paradoxical that no hydrolysis was observed after completion of the mechanochemical synthesis, where hygroscopic potassium fluoride was mixed with easily hydrolysable transition metal fluorides in air.[61]

In many photographs, fluoride nanoobjects look like clouds and pieces of cotton without pronounced boundaries. This is a characteristic feature of a fractal structure.[237, 238] The self-similarity of the particle shape at several structural levels was noted.[86] This problem calls for further investigation. It should be noted that the term 'surface area' for fractals is ambiguous (can be determined in different ways) and depends on the measurement procedure. In particular, different values of the specific surface area, which is the practically important parameter (for example, for catalysts), can be obtained by the adsorption method with the use of different adsorbed gases.

The random arrangement of fluoroaluminate octahedra postulated in a fluoride gel (see Fig. 6) corresponds to a network in fluoroaluminate glasses. Therefore, one would expect that analogous gels would be prepared for other groups of fluoride glasses, such as fluoroberyllate, fluorohafnate, fluorozirconate and fluoroindate glasses. Amorphous fluoride powders prepared by the sol–gel technology hold considerable promise for the synthesis of different types of fluoride glasses.

Nanofluorides are promising materials for the synthesis of single crystals, particularly, if the components of compounds are substantially different in volatility. An example is $SrAlF_5$ single crystals of which are promising nonlinear optical materials for laser frequency conversion to the UV range.[22]

High mobility of fluoride ions, which is probable in fluoride nanoparticles, may be of practical importance.[64] It should be noted that ^{19}F NMR spectroscopy is the method of choice for studying this phenomenon.[44]

It is also necessary to examine the dependence of the toxic effect of fluorides on the particle size.

We thank J Ballato, A Bednarkiewicz, A I Boltalin, J Botta, D Boyer, I I Buchinskaya, V M Buznik, E E Carpenter, Y Chunhua, M Dejneka, A Fery, W Filho, S Fumio, T I Glazunova, R N Grass, C L Griffiths, M G Ivanov, Ishizawa Hitoshi, E Kemnitz, R N Kostoff, Y D Li, J L Light,

M Lezhnina, R Mahiou, J-M Nedelec, O B Petrova, L Prentice, B P Sobolev, W J Stark, N Stubicar, M Tyas, F van Veggel, Xianping Fan, Xianwen Wei, Yuhua Wang, Qiwu Zhang, Jishuang Zhang and P Zipper for providing information. We thank E V Chernova for technical help in preparing the manuscript.

This review has been written with the financial support of the Government Contract of the Ministry of Education and Sciences (No 02.435.11.2011, 15 July 2005).

References

1. Y Gogotsi (Ed.) *Nanomaterials Handbook* (London: Taylor Francis, 2006)
2. B L Cushing, V L Kolesnichenko, Ch J O'Connor *Chem. Rev.* **104** 3893 (2004)
3. J Lu, M Prabhu, J Song, C Li, J Xu, K Ueda, A Kaminskii, H Yagi, T Yanagitani *Appl. Phys. B* **71** 469 (2000)
4. J Lu, K Ueda, H Yagi, T Yanagitani, Y Akiyama, A Kaminskii *J. Alloys Compd.* **341** 220 (2002)
5. I Hitoshi, in *Proceedings of the 13th International Workshop on Sol–Gel Sciences and Technology, Los Angeles, CA, 2005* p. 289
6. R N Grass, W J Stark *Chem. Commun.* 1767 (2005)
7. P P Fedorov, V V Osiko, T T Basiev, Yu V Orlovskii, S Vasil'ev, V V Voronov, S V Lavrishchev, S V Kuznetsov, E A Tkachenko, V A Konyushkin, E Belyaev, I A Mironov, V A Demidenko, M Sh Akchurin, I V Yarotskaya *Otchet o Nauchno-issledovatel'skoi Rabote po Gosudarstvennomu Kontraktu 02.435.11.2011* (Report about Research on State Contract 02.435.11.2011) (Moscow: Department of Education and Science, 2005)
8. M Sh Akchurin, R V Gainutdinov, P L Smolyanskii, P P Fedorov *Dokl. Akad. Nauk* **406** 180 (2006) [a]
9. R S Meltzer, W M Yen, H Zheng, S P Feofilov, M J Dejneka *Phys. Rev. B* **66** 224202 (2002)
10. S P Feofilov, Doctoral Thesis in Physicomathematical Sciences, Ioffe Physico-Technical Institute, St Petersburg, 2004
11. A Bednarkewicz, A Mech, M Karbowiak *J. Lumin.* **114** 247 (2005)
12. V Sudarsan, F C J M van Veggel, R A Herring, M Raudsepp *J. Mater. Chem.* **15** 1332 (2005)
13. V Sudarsan, S Sivakumar, F C J M van Veggel *Chem. Mater.* **17** 4736 (2005)
14. M Karbowiak, A Mech, A Bednarkiewicz, W Strek *J. Alloys Compd.* **380** 321 (2004)
15. S Sivakumar, F C J M van Veggel *J. Am. Chem. Soc.* **127** 12464 (2005)
16. T S Koroleva, M M Kidibaev, B K Dzholdoshov, C Pedrini, B Hautefeuille, K Lebbou, O Tillement, J-M Fourmigue, B V Shul'gin, A N Cherepanov, V I Solomonov, M G Ivanov *Fiz. Tv. Tela* **47** 1417 (2005) [b]
17. E Kemnitz, U Gross, S Rudiger, C S Shekar *Angew. Chem., Int. Ed.* **42** 4251 (2003)
18. J K Murthy, U Gross, S Rudiger, E Kemnitz *Appl. Catal., A* **278** 133 (2004)
19. T Krahl, E Kemnitz *Angew. Chem., Int. Ed.* **43** 6653 (2004)
20. J K Murthy, U Gross, S Rudiger, E Unveren, W Unger, E Kemnitz *Appl. Catal., A* **282** 85 (2005)
21. T Yu Glazunova, Candidate Thesis in Chemical Science, Moscow State University, Moscow, 2005
22. S Fujihara, S Ono, Y Kishiki, M Tada, T Kimura *J. Fluorine Chem.* **105** 65 (2000)
23. US P. 0121235 (2004)
24. M Markovic, S Frukhtbeyn, S Takagi, L C Chow, in *The IADR/AADR/CADR of the 80th General Session of the International Association of Dental Research, San Diego, CA, 2002*
25. K J Cross, N L Huq, D P Stanton, M Sum, E C Reynolds *Biomaterials* **25** 5061 (2004)
26. L H Prentice, M J Tyas, M F Burrow *Dent. Mater.* **22** 746 (2006)
27. N Martin, P Boutinaud, R Mahiou, J-C Cousseins, M Bouderbala *J. Mater. Chem.* **9** 125 (1999)
28. M Karbowiak, A Mech, A Bednarkiewicz, W Strek *J. Lumin.* **114** 1 (2005)
29. P P Fedorov, V V Osiko, in *Bulk Crystal Growth of Electronic, Optical and Optoelectronic Materials* (Ed. P Capper) (San Diego, CA: Wiley, 2005) p. 339
30. E G Rakov, V V Teslenko *Pirogidroliz Neorganicheskikh Ftoridov* (Pyrohydrolysis of Inorganic Fluorides) (Moscow: Energoatomizdat, 1987)
31. L Domange *Ann. Chim. (Paris)* **7** 225 (1937)
32. J C Warf, W C Cline, R D Tevebaugh *Anal. Chem.* **26** 342 (1954)
33. C V Banks, K E Burke, J W O'Laughlin *Anal. Chim. Acta* **19** 230 (1958)
34. D R Messier *J. Electrochem. Soc.* **115** 397 (1968)
35. Y Susumu, J-H Kim, M Takashima *Solid State Sci.* **4** 1481 (2002)
36. T Inagaki, Y Yoshimura, Y Kanda, Y Matsumoto, K Minami *Nucl. Instrum. Methods Phys. Res., A* **443** 126 (2000)
37. M A Mikhailov, E P Ozhigov *Soobsh. Dal'nevostoch. Filiala SO Akad. Nauk SSSR* (9) 13 (1958)
38. P P Fedorov, O S Bondareva, V A Stasyuk, M D Skorokhvatov, B P Sobolev, P I Fedorov *Zh. Neorg. Khim.* **42** 698 (1997) [c]
39. R Lebullenger, M Poulain *J. Non-Cryst. Solids* **184** 166 (1995)
40. S J Gregg, K S W Sing *Adsorption, Surface Area and Porosity* (2nd Ed.) (London: Academic Press, 1982)
41. G K Borisov, S L Vershinin, S G Chugunova, M F Churbanov *Vysokochist. Veshchestva* (4) 75 (1993)
42. R C Pastor *J. Cryst. Growth* **203** 421 (1999)
43. P Thangadurai, S Ramasamy, R Kesavamorthy *J. Phys.: Condens. Matter* **17** 863 (2005)
44. W Puin, P Heitjans *Nanostruct. Mater.* **6** 885 (1995)
45. G G Lepeshkov, A O Larina, A P Dudka, A S Avilov, B P Sobolev, in *Tezisy Dokladov V Natsional'noi Konferentsii po Primeneniyu Rentgenovskogo, Sinkhrotronnogo Izluchenii, Neitronov i Elektronov dlya Issledovaniya Nanomaterialov i Nanosistem* (Abstracts of Reports of the Vth National Conference on Application of X-ray, Synchrotron Radiation, Neutrons and Electrons for Investigation of Nanomaterials and Nanosystems) (Moscow: A V Shubnikov Institute of Crystallography, Russian Academy of Sciences, 2005) p. 229
46. B Bureau, H Guérault, G Silly, J Y Buzaré, J M Grenècche *J. Phys.: Condens. Matter* **11** 423 (1999)
47. H Guérault, J M Greneche *J. Phys.: Condens. Matter* **12** 4791 (2000)
48. S Fujihara, S Koji, Y Kadota, T Kimura *J. Am. Ceram. Soc.* **87** 1959 (2004)
49. M M Lezhnina, H Kätker, U H Kynast *Fiz. Tv. Tela* **47** 1423 (2005) [b]
50. R M Zakalyukin, A I Boltalin, N G Furmanova, S I Troyanov, in *II Natsional'naya Kristallokhimicheskaya Konferentsiya (Tez. Dokl.), Chernogolovka, 2000* [The IInd National Crystallographic Conference (Abstracts of Reports), Chernogolovka, 2000] p. 125
51. N G Zhuravleva, A A Eliseev, N A Sapoletova, A V Lukashin, U Kynast, Yu D Tretyakov *Mater. Sci. Eng. C* **25** 549 (2005)
52. T Yu Glazunova, A I Boltalin, P P Fedorov *Zh. Neorg. Khim.* **51** 1061 (2006) [c]
53. L J Lingg, A D Berry, A P Purdy, K J Ewing *Thin Solid Films* **209** 9 (1992)
54. J A Samuels, K Folting, J C Huffman, K G Caulton *Chem. Mater.* **7** 929 (1995)
55. G G Condorelli, S Gennaro, I L Fragata *Chem. Vap. Deposition* **7** 151 (2001)
56. O Poncelet, J Guilment, D Martin *J. Sol-Gel Sci. Technol.* **13** 129 (1998)
57. B Huang, Zh Liu, J-M Hong, X-T Chen, Z-L Xue, X-Z You *J. Cryst. Growth* **276** 613 (2005)
58. E Avvakumov, M Senna, N Kosova *Soft Mechanochemical Synthesis: A Basis for New Chemical Technologies* (Boston: Kluwer Academic, 2001)
59. J Lu, Q Zhang, F Saito *Chem. Lett.* **31** 1176 (2002)
60. J Lee, W Zhang, F Saito *J. Am. Ceram. Soc.* **84** 863 (2001)
61. J Lee, Q Zhang, F Saito *J. Alloys Compd.* **348** 214 (2003)
62. Jg Lee, H Shin, Jn Lee, H Chung, Q Zhang, F Saito *Mater. Trans., JIM* **44** 1457 (2003)

63. B P Sobolev, I A Sviridov, V I Fadeeva, S N Sul'yanov, N I Sorokin, Z I Zhmurova, P Erero, A Landa-Kanovas, R M Rokhas *Kristallografiya* **50** 536 (2005) [d]
64. M Kumar, S S Sekhon *J. Phys. D* **34** 2995 (2001)
65. A R Yavari, A LeMoulec, J F R de Castro, S Deledda, O Friedrichs, W J Botta, G Vaughan, T Klassen, A Fernandez, A Kvick *Scr. Mater.* **52** 719 (2005)
66. D R Leiva, J F R de Castro, T T Ishikawa, W J Botta, in *Proceedings of the 5th International Latin – American Conference on Powder Technology, Costa do Sauipe, Brazil, 2005* P 05/06
67. S Deledda, A Borissova, C Poinsignon, W J Botta, M Dornheim, T Klassen *J. Alloys Compd.* **404 – 406** 409 (2005)
68. B P Sobolev *The Rare Earth Trifluorides. The High-temperature Chemistry of the Rare Earth Trifluorides* (Barcelona: Institut d'Estudis Catalans, 2000) Pt. 1
69. L R Batsanova, L M Yankovskaya, L V Lukina *Zh. Neorg. Khim.* **17** 1258 (1972) [c]
70. B N Ivanov-Emin, V A Zaitseva, A I Ezhov *Zh. Neorg. Khim.* **12** 1343 (1967) [c]
71. L R Batsanova, V P Doronina, N V Podberezskaya *Izv. Sib. Otd. Akad. Nauk, Ser. Khim. Nauk* **4** (2) 41 (1968)
72. R K Narasinmba, M A H Shareef *J. Mater. Sci. Lett.* **2** 83 (1983)
73. M Shareefuddin, M Narasimha Chary *J. Alloys Compd.* **218** 121 (1995)
74. E I Mel'nichenko, T A Kalacheva, S A Polishchuk, in *VII Vsesoyuznaya Konferentsiya po Khimii i Tekhnologii Redkikh i Rasseyannykh Elementov (Tez. Dokl.), Apatity, 1988* [The VIIth All-Union Conference on Chemistry and Technology of Rare and Scattered Elements (Abstracts of Reports), Apatity, 1988] p. 39
75. A Mech, M Karbowiak, L Kepinski, A Bednarkiewicz, W Strek *J. Alloys Compd.* **380** 315 (2004)
76. P P Fedorov *Zh. Neorg. Khim.* **44** 1791 (1999) [c]
77. P P Fedorov, B P Sobolev *Kristallografiya* **37** 1210 (1992) [d]
78. M Wang, Q-L Huang, J-M Hong, W-H Wu, Z Yu, X-T Chen, Z-L Xue *Solid State Commun.* **136** 210 (2005)
79. R E Thoma, H Insley, G M Hebert *Inorg. Chem.* **5** 1222 (1966)
80. P P Fedorov, V B Aleksandrov, O S Bondareva, I I Buchinskaya, M D Val'kovskii, B P Sobolev *Kristallografiya* **46** 280 (2001) [d]
81. V Sudarsan, F C J M Veggel, R A Herring, M Raudsepp, in *Proceedings of the 87th Canadian Chemistry Conference and Exhibition, London, ON, Canada, 2004* Poster 676
82. P R Diamente, R D Burke, F C J M Veggel *Langmuir* **22** 1782 (2006)
83. Ja W Stouwdam, F C J M Veggel *Langmuir* **20** 11763 (2004)
84. C Sassoye, A De Kozak, M Mortier, in *Proceedings of the 13th International Workshop on Sol – Gel Sciences and Technology, Los Angeles, CA, 2005* p. 549
85. N Stubicar *Cryst. Growth Des.* **5** 113 (2005)
86. N Stubicar, M Stubicar, P Zipper, B Chernev *Cryst. Growth Des.* **5** 123 (2005)
87. S Heer, K Kompte, H-U Gudel, M Haase *Adv. Mater.* **16** 2102 (2004)
88. B P Sobolev, D A Mineev, V P Pashutin *Dokl. Akad. Nauk SSSR* **150** 791 (1963) [e]
89. L R Batsanova, L Yu Kravchenko, N V Podberezskaya, L A Baidina *Izv. Akad. Nauk SSSR, Neorg. Mater.* **10** 1979 (1974) [e]
90. K Yanasigawa, M Yoshimura, S Somiya *Nippon Kagaku Kaishi* **9** 1382 (1981)
91. L N Demianets *Prog. Cryst. Growth Charact. Mater.* **21** 299 (1990)
92. N M Khaidukov, P P Fedorov, L N Dem'yanets, I P Zibrov, V A Malyusov *Zh. Neorg. Khim.* **35** 679 (1990) [c]
93. N M Khaidukov, P P Fedorov, N A Abramov *Izv. Akad. Nauk SSSR, Neorg. Mater.* **27** 2614 (1991) [f]
94. C Zhao, S Feng, R Xu, C Shi, J Ni *J. Chem. Soc., Chem. Commun.* 945 (1994)
95. X Wang, Y Li *Angew. Chem.* **42** 3497 (2003)
96. X Wang, Y Li *Chem. – Eur. J.* **9** 5627 (2003)
97. G De, W Qin, J Zhang, D Zhao, J Zhang *Chem. Lett.* **34** 7 (2005)
98. Y Ruoxue, Y Li *Adv. Funct. Mater.* **15** 763 (2005)
99. US P. 6316377 (2001)
100. US P. 6667019 (2003)
101. B Huang, J-M Hong, X-T Chen, Z-L Xue, X-Z You *J. Cryst. Growth* **276** 491 (2005)
102. M Zhang, Z Wang, M Mo, X Chen, R Zhang, W Yu, Y Qian *Mater. Chem. Phys.* **89** 373 (2005)
103. S Eiden-Assmann, G Maret *Mater. Res. Bull.* **39** 21 (2004)
104. S Fujihara, C Mochizuki, T Kimura *J. Non-Cryst. Solids* **244** 267 (1999)
105. M Nagai, T Nishino *Solid State Ionics* **99** 221 (1997)
106. T P Hoar, J H Schulman *Nature (London)* **152** 102 (1943)
107. J H Schulman, D P Riley *J. Colloid Sci.* **3** 383 (1948)
108. M Boutonnet, J Kizling, P Stenius, G Maire *Colloids Surf.* **5** 209 (1982)
109. M Roth, R Hempelmann, O Borgmeier, T Eifert, H Lueken *Nanostruct. Mater.* **12** 855 (1999)
110. C J O'Connor, V Kolesnichenko, E Carpenter, C Sangregorio, W Zhou, A Kumbhar, J Sims, F Agnoli *Synth. Met.* **122** 547 (2001)
111. E E Carpenter Ph.D. Thesis University of New Orleans, New Orleans, LA, 1999
112. C M Bender, J M Burlitch *Chem. Mater.* **12** 1969 (2000)
113. R Hua, C Zang, C Shao, D Xie, C Shi *Nanotechnology* **14** 588 (2003)
114. S Qiu, J Dong, G Chen *Powder Technol.* **113** 9 (2000)
115. H Lian, J Liu, Z Ye, C Shi *Chem. Phys. Lett.* **386** 291 (2004)
116. H Lian, M Zhang, J Liu *Chem. Phys. Lett.* **395** 362 (2004)
117. H Lian, J Liu, Z Ye, C Shi *J. Rare Earth* **22** 67 (2004)
118. H Lian, Z Ye, C Shi *Nanotechnology* **15** 1455 (2004)
119. H Lian, J Liu, Z Ye, C Shi *J. Nanosci. Nanotechnol.* **5** 394 (2005)
120. H K Henisch *Crystal Growth in Gel* (University Park, London: The Pennsylvania State University Press, 1970)
121. K-Th Wilke *Kristallzuchtung* (Berlin: VEB Deutscher Verlag der Wissenschaften, 1973)
122. P J Melling, M A Thomson *J. Mater. Res.* **5** 1092 (1990)
123. R E Riman, M Dejneka, J Eamsiri, E Snitzer, A Mailhot, A Leaustic *J. Sol-Gel Sci. Technol.* **2** 849 (1994)
124. A A Rywak, J M Burlitch *Chem. Mater.* **8** 60 (1996)
125. S Fujihara, M Tada, T Kimura *J. Sol-Gel Sci. Technol.* **19** 311 (2000)
126. S Lepoutre, D Boyer, R Mahiou *Opt. Mater.* **28** 592 (2006)
127. D Boyer, H Kharbache, R Mahiou *Opt. Mater.* **28** 53 (2006)
128. S Fujihara, Y Kishiki, T Kimura *J. Alloys Compd.* **333** 76 (2002)
129. P Gredin, L Jessica *Solid State Sci.* **6** 1221 (2004)
130. Eur. P. 1 008 555 B9 (1999)
131. S Fujihara, T Kato, T Kimura *J. Am. Ceram. Soc.* **84** 2716 (2001)
132. A Biswas, G S Maciel, C S Friend, P N Prasad *J. Non-Cryst. Solids* **316** 393 (2003)
133. E Kemnitz, S Ruediger, U Gross *Z. Anorg. Allg. Chem.* **630** 1696 (2004)
134. S K Ruediger, U Gross, M Feist, H A Prescott, C S Shekar, S I Troyanov, E Kemnitz *J. Mater. Chem.* **15** 588 (2005)
135. K Takeuchi, Y Kuga *J. Aerosol Sci.* **28** S343 (1997)
136. K Takeuchi, Y Kuga, S Satooka, K Okuyama *J. Aerosol Sci.* **29** 1027 (1998)
137. M Hirasava, Y Kuga, T Seto, K Okuyama, K Takeuchi *Appl. Phys. A* **74** 513 (2002)
138. M Mortier, G Patriarche *Opt. Mater. (Amsterdam)* **28** 1401 (2006)
139. G V Berezhkova *Nitevidnye Kristally* (Filamentary Crystals) (Moscow: Nauka, 1969)
140. A A Chernov, E I Givargizov, Kh S Bagdasarov *Sovremennaya Kristallografiya* (Modern Crystallography) (Moscow: Nauka, 1980) Vol. 3
141. I I Buchinskaya, B P Sobolev, in *Shestaya Mezhdunarodnaya Konferentsiya 'Rost Kristallov i Teploperenos' (Sbornik Trudov), Obninsk, 2005* (Proceedings of the Sixth International Conference 'Growth of Crystals and Heat Transmission', Obninsk, 2005) Vol. 1, p. 160
142. M Cao, C Hu, E Wang *J. Am. Chem. Soc.* **125** 11196 (2003)
143. A Golubovic, J Fitzgerald, I Berman, J Bruce, R Bradbury, J J Comer, W S Ewing, H G Lipson *U.S. Dept. Commer. Natl. Bur. Stand. Spec. Publ.* **462** 271 (1976)

144. G Hass, M Francombe, R Hoffman (Eds) *Physics of Thin Films: Advances in Research and Development Series* Vol. 8 (New York: Academic Press, 1975)
145. M Ya Khodos, A A Golota, Yu F Zhuravlev, L V Limanskaya *Neorg. Mater.* **27** 607 (1991) [f]
146. A F Golota, Doctoral Thesis in Chemical Science, Saratov State University, Saratov, 1999
147. C J Palmstrom *Annu. Rev. Mater. Sci.* **25** 389 (1995)
148. E Doran, L E Bausa, R Legros, C Fontaine *Solid State Commun.* **94** 379 (1995)
149. J M Ko, T Fukuda *J. Cryst. Growth* **200** 490 (1999)
150. A El Fajri, M Moussetad, P Tardy, A S Barriere *Phys. Status Solidi A* **179** 373 (2000)
151. C Dujardin, C Pedrini, N Garnier, A N Belsky, K Lebbou, J M Ko, T Fukuda *Opt. Mater. (Amsterdam)* **16** 69 (2001)
152. M Vijayakumar, S Selvasekarapandian, T Gnanasekaran, S Fujihara, S Koji *J. Fluorine Chem.* (2006) (in the press)
153. C L Griffiths, J E MacDonald, R H Williams *Appl. Surf. Sci.* **56–58** 782 (1992)
154. L C Jenkins, C L Griffiths, A Hughes, J Richards, R H Williams *J. Vac. Sci. Technol., B* **11** 1541 (1993)
155. P P Fedorov, Doctoral Thesis in Chemical Science, Moscow Institute of Fine Chemical Technology, Moscow, 1991
156. N S Sokolov, N N Faleev, S V Gastev, L Yakovlev *J. Vac. Sci. Technol., A* **13** 2703 (1995)
157. V A Rozhkov, M B Shalimova *Semiconductors* **33** 731 (1999)
158. M Malac, M Schoefield, Y Zhu *J. Appl. Phys.* **92** 1112 (2002)
159. G B Thompson, D D Allred *J. X-Ray Sci. Technol.* **7** 159 (1997)
160. J Ballato, R E Riman, E Snitzer *J. Non-Cryst. Solids* **213–214** 126 (1997)
161. S Fujihara, M Tada, T Kimura *Thin Solid Films* **304** 252 (1997)
162. M Tada, S Fujihara, T Kimura *J. Mater. Res.* **14** 1610 (1999)
163. S Fujihara, Y Kadota, T Kimura *J. Sol-Gel Sci. Technol.* **24** 147 (2002)
164. W Pannhorst *J. Non-Cryst. Solids* **219** 198 (1997)
165. P A Tick, N F Borelli, L K Cornelius, M A Newhouse *J. Appl. Phys.* **78** 6367 (1995)
166. P A Tick *Opt. Lett.* **23** 1904 (1998)
167. P A Tick, N F Borelli, I M Reaney *Opt. Mater. (Amsterdam)* **15** 81 (2000)
168. S Tanabe, H Hayashi, T Hanada, N Onodera *Opt. Mater. (Amsterdam)* **19** 343 (2002)
169. F Goutaland, P Jander, W S Brocklesby, D Goujun *Opt. Mater. (Amsterdam)* **22** 383 (2003)
170. R S Meltzer, H Zheng, M J Dejneka *J. Lumin.* **107** 166 (2004)
171. M J Dejneka *J. Non-Cryst. Solids* **239** 149 (1998)
172. M En, Z Hu, Y Wang, F Bao *J. Lumin.* **118** 131(2005)
173. S Tanabe, H Hayashi, T Hanada *J. Am. Ceram. Soc.* **85** 839 (2002)
174. M Beggiora, I M Reaney, A B Seddon, D Furniss, S A Tikhomirova *J. Non-Cryst. Solids* **326–327** 476 (2003)
175. W Glass, J Toulouse, P A Tick *J. Non-Cryst. Solids* **222** 258 (1997)
176. V K Tikhomirov, D Furniss, A B Seddon *Appl. Phys. Lett.* **81** 1937 (2002)
177. J B Qiu, Y Kawamoto, J J Zhang *J. Appl. Phys.* **92** 5163 (2002)
178. D Chen, Y Wang, Y Yu, M En, F Bao, Z Hu, Y Chen *Mater. Chem. Phys.* **95** 264 (2006)
179. F C Guinhos, P C Nobrega, P A Santa-Cruz *J. Alloys Compd.* **323–324** 358 (2001)
180. R Dekker, V Sudarsan, F C J M Veggel, K Wörhoff, A Driessen, in *Proceedings of the Symposium IEEE/LEOS Benelux Chapter, Ghent, 2004* p. 295
181. H Gleiter *Acta Mater.* **48** 1 (2000)
182. A A Lebedev *Izbrannye Trudy* (Selected Works) (Leningrad: Nauka, 1974) p. 286
183. W H Zachariasen *J. Am. Chem. Soc.* **54** 3841 (1932)
184. B E Warren *J. Appl. Phys.* **8** 645 (1937)
185. B E Warren *J. Am. Ceram. Soc.* **24** 256 (1941)
186. E A Porai-Koshits *J. Non-Cryst. Solids* **123** 7 (1990)
187. G N Greaves *J. Non-Cryst. Solids* **71** 203 (1985)
188. V M Buznik *Yadernaya Spektroskopiya Neorganicheskikh Ftoridov* (Nuclear Spectroscopy of Inorganic Fluorides) (Vladivostok: Dal'nauka, 1997)
189. C H L Goodman *Phys. Chem. Glasses* **26** 1 (1985)
190. J Lucas *J. Fluorine Chem.* **72** 177 (1995)
191. P P Fedorov *Kristallografiya* **42** 1141 (1997) [d]
192. P P Fedorov *Neorg. Mater.* **33** 1415 (1997) [e]
193. P P Fedorov, R M Zakalyukin, L N Ignat'eva, V M Buznik *Usp. Khim.* **69** 767 (2000) [*Russ. Chem. Rev.* **69** 705 (2000)]
194. R M Zakalyukin, P P Fedorov *Neorg. Mater.* **39** 756 (2003) [f]
195. M Baricco, L Battezzatti, M Braglia, G Cocito, M Gava, J Kraus, S Mosso *J. Non-Cryst. Solids* **213–214** 79 (1997)
196. D R MacFarline, J Javorniczky, P J Newman *J. Non-Cryst. Solids* **256–257** 366 (1999)
197. S Schweizer, S Assmann, M Secu, A Edgar, J-M Spaeth *Radiat. Meas.* **33** 487 (2001)
198. S J L Ribeiro, Ph Goldner, F Auzel *J. Non-Cryst. Solids* **219** 176 (1997)
199. V D Fedorov, V V Sakharov, P B Baskov, A M Provorova, M F Churbanov, V G Plotnichenko, P Kh Ioakhim, P Marsel', I Kirkhof, I Kobelka *Ros. Khim. Zh.* **45** 51 (2001) [g]
200. W A Pisarka, J Pisarka, T Goryczka, G Domoniak-Dzik, W Ruba-Romanowski *J. Alloys Compd.* **398** 272 (2005)
201. M Mortier, A Monteville, G Patriarche, G Maze, F Auzel *Opt. Mater. (Amsterdam)* **16** 255 (2001)
202. L Anselm, G H Frischat *J. Non-Cryst. Solids* **213–214** 375 (1997)
203. T M Turkina, Candidate Thesis in Physical and Mathematical Sciences, Institute of Crystallography, Academy of Sciences, Moscow, 1990
204. B P Sobolev, A M Golubev, P Errero *Kristallografiya* **48** 148 (2003) [d]
205. P P Fedorov *Russ. J. Inorg. Chem.* **45** (Suppl. 3) S268 (2000)
206. V V Osiko *Lazernye Materialy. Izbrannye Trudy* (Laser Materials. Selected Works) (Moscow: Nauka, 2002)
207. A M Prokhorov, V V Osiko, in *Problemy Sovremennoi Kristallografii* (The Problems of Current Crystallography) (Moscow: Nauka, 1975) p. 280
208. P P Fedorov *Bull. Soc. Cat. Cien.* **12** 349 (1991)
209. E A Sul'yanova, A P Shcherbakov, V N Molchanov, V I Simonov, B P Sobolev *Kristallografiya* **50** 235 (2005) [d]
210. O Greis, J M Haschke, in *Handbook on the Physics and Chemistry of Rare Earth* Vol. 5 (Eds K A Gscheidner, L Eyring) (Amsterdam, New York, Oxford: Elsevier, 1982) p. 387
211. S A Kazanskii, in *Spektroskopiya Kristallov* (Spectroscopy of Crystals) (Leningrad: Nauka, 1989) p. 110
212. M Svantner, E Mariani, P P Fedorov, B P Sobolev *Cryst. Res. Technol.* **16** 617 (1981)
213. A K Ivanov-Shits, N I Sorokin, P P Fedorov, B P Sobolev *Solid State Ionics* **31** 253 (1989)
214. M Tromel *Z. Kristallogr.* **183** 15 (1988)
215. Yu D Tretyakov *Neorg. Mater.* **21** 693 (1985) [f]
216. P P Fedorov *Kondens. Sredy Mezhfaz. Granitsy* **4** 346 (2002)
217. B Chalmers *Teoriya Zatverdevaniya* (The Theory of Freezing) (Moscow: Metallurgiya, 1968)
218. V Trnovcova, V Labas, P P Fedorov, M Yu Starostin, in *Solid State Ionics: Science and Technology. Microstructure and Physical Properties of Superionic Eutectic Composites Prepared from Melt* (Singapore, New Jersey, London, Hong Kong: World Scientific Publ., 1998) p. 325
219. P P Fedorov, I I Buchinskaya, N A Ivanovskaya, V V Konovalova, S V Lavrishchev, B P Sobolev *Dokl. Akad. Nauk* **401** 652 (2005) [e]
220. N Sata, N Y Jin-Phillipp, K Eberl, J Maier *Solid State Ionics* **154** 497 (2002)
221. H Naito, S Fujihara, T Kimura *J. Sol-Gel Sci. Technol.* **26** 997 (2003)
222. S Fujihara, H Naito, T Kimura *Thin Solid Films* **389** 227 (2001)
223. J J Maier *J. Phys. Chem. Solids* **46** 309 (1985)
224. J J Maier *Angew. Chem., Int. Ed. Engl.* **32** 313 (1993)
225. A B Yaroslavtsev *Russ. J. Inorg. Chem.* **45** (Suppl. 3) S249 (2000)
226. S Fujitsu, M Miyayama, K Kuomoto, H Yanagida, T Kanazawa *J. Mater. Sci.* **20** 2103 (1985)
227. R Akila, K T Jacob *Solid State Ionics* **25** 217 (1987)
228. Yu A Panshin, S G Malkevich, I S Dunaevskaya *Ftoroplasty* (Fluoroplastics) (Leningrad: Khimiya, 1978)

229. V M Buznik, V M Fomin, A P Alkhimov, L I Ignat'eva, A K Tsvetnikov, V G Kuryavyi, V F Kosarev, S P Gubin, O I Lomovskii, A A Okhlopkova, N F Uvarov, S V Klinkov, I I Shabalin *Metallopolimernye Nanokompozity (Poluchenie, Svoistva, Primenenie)* (Metal-polymeric Nanocomposites (Production, Properties and Applications) (Novosibirsk: Siberian Branch of the Russian Academy of Sciences, 2005)
230. S P Gubin, M S Korobov, G Yu Yurkov, A K Tsvetnikov, V M Buznik *Dokl. Akad. Nauk* **388** 493 (2003) [a]
231. M S Korobov, G Yu Yurkov, A V Kozinkin, Yu A Koksharov, I V Pirog, S V Zubkov, V V Kitaev, D A Sarychev, V M Buznik, A K Tsvetnikov, S P Gubin *Neorg. Mater.* **40** 31 (2004) [f]
232. M S Korobov, Candidate Thesis in Chemical Sciences, Institute of General and Inorganic Chemistry, Russian Academy of Sciences, Moscow, 2004
233. F Dubreuil, D G Shchukin, G B Sukhorukov, A Fery *Macromol. Rapid Commun.* **25** 1078 (2004)
234. F Wang, Y Zhang, X Fan, M Wang *Nanotechnology* **17** 1527 (2006)
235. G Yi, H Lu, S Zhao, Y Ge, W Yang, D Chen, L-H Guo *Nano Lett.* **4** 11 2191 (2004)
236. X-W Wei, J Xu, X-J Song, Y-H Ni, P Zhang, C-J Xia, G-C Zhao, Z-S Yang *Mater. Res. Bull.* **41** 92 (2006)
237. B B Mandelbrot *The Fractal Geometry of Nature* (New York: W H Freeman and Company, 1977)
238. J Feder *Fractals* (New York: Plenum, 1988)

[a] — *Dokl. Phys. (Engl. Transl.)*
[b] — *Phys. Solid State (Engl. Transl.)*
[c] — *Russ. J. Inorg. Chem. (Engl. Transl.)*
[d] — *Crystallogr. Rep. (Engl. Transl.)*
[e] — *Dokl. Chem. (Engl. Transl.)*
[f] — *Inorg. Mater. (Engl. Transl.)*
[g] — *Mendeleev Chem. J. (Engl. Transl.)*